

2014

# Aromatic Superhalogens

Brandon Child

*Virginia Commonwealth University*

Santanab Giri

*Virginia Commonwealth University*

Scott Gronert

*Virginia Commonwealth University, sgronert@vcu.edu*

Puru Jena

*Virginia Commonwealth University, pjena@vcu.edu*

Follow this and additional works at: [http://scholarscompass.vcu.edu/phys\\_pubs](http://scholarscompass.vcu.edu/phys_pubs)

 Part of the [Physics Commons](#)

Copyright © 2014 WILEY-VCH Verlag GmbH & Co. KGaA, Weinheim. This is the peer reviewed version of the following article: Child, B. Z., Giri, S., Gronert, S. and Jena, P. (2014), Aromatic Superhalogens. *Chem. Eur. J.*, 20: 4736–4745. doi: 10.1002/chem.201305057, which has been published in final form at <http://dx.doi.org/10.1002/chem.201305057>. This article may be used for non-commercial purposes in accordance with Wiley Terms and Conditions for self-archiving.

Downloaded from

[http://scholarscompass.vcu.edu/phys\\_pubs/7](http://scholarscompass.vcu.edu/phys_pubs/7)

This Article is brought to you for free and open access by the Dept. of Physics at VCU Scholars Compass. It has been accepted for inclusion in Physics Publications by an authorized administrator of VCU Scholars Compass. For more information, please contact [libcompass@vcu.edu](mailto:libcompass@vcu.edu).

# Aromatic Superhalogens

Brandon Z. Child<sup>1</sup>, Santanab Giri<sup>1</sup>, Scott Gronert<sup>2</sup>, and Puru Jena\*<sup>1</sup>

<sup>1</sup>Physics Department, Virginia Commonwealth University, Richmond, VA 23284

<sup>2</sup>Chemistry Department, Virginia Commonwealth University, Richmond, VA 23284

## Abstract

No organic molecules with electron affinities near or above those of halogens are known. We show for the first time that aromaticity rules can be used to design molecules with electron affinities far exceeding those of halogen atoms either by tailoring the ligands of cyclopentadienyl or by multiple benzo-annulations of cyclopentadienyl in conjunction with the substitution of CH groups with isoelectronic N atoms. Results based on density functional theory reveal that the electron affinities of some of these organic molecules can reach as high as 5.59 eV, thus opening the door to new class of superhalogens that contain neither a metal nor a halogen atom.

\*pjena@vcu.edu

**Key words:** superhalogens, aromatic molecules, electron affinity, electro negative species

## I. Introduction

Superhalogens are a class of molecules whose electron affinities are larger than that of any halogen atom. As a result superhalogens not only form stable salts but, due to the strong oxidizing properties of their parent species, also play a major role in the synthesis of new compounds. Consequently, there is a growing interest in a fundamental understanding of the structure, stability, and properties of these molecules and finding ways to enlarge their scope. For example, superhalogens were originally conceived<sup>[1]</sup> to have a metal atom, M, at the core surrounded by halogen atoms, X, whose number exceed the maximal valence,  $k$  of the metal atom by one, namely  $\text{MX}_{k+1}$ . In the 80's and 90's many superhalogens were designed by considering simple metal atoms ( $\text{M}=\text{Li}, \text{Na}, \text{Mg}, \text{Al}, \dots$ ) at the core and halogen atoms ( $\text{X}=\text{F}, \text{Cl}$ ) as ligands<sup>[2-5]</sup>. The first experimental proof of the superhalogens came from Wang's group in 1999<sup>[6]</sup>. Since then a considerable amount of work has been done to design and synthesize new superhalogens and understand their atomic structure and properties<sup>[7-13]</sup>. These include superhalogens with transition metal atoms at the core<sup>[14]</sup>, and/or O,  $\text{NO}_3$ , CN,  $\text{BH}_4$ , and  $\text{BF}_4$  moieties as ligands<sup>[15-19]</sup>. Superhalogens such as borane derivatives that contain neither a metal nor a halogen atom have also been designed<sup>[20]</sup>. In addition, it was recently shown<sup>[21]</sup> that a new class of highly electronegative ions can form if superhalogens instead of halogens are used as ligands. These new species called hyperhalogens have electron affinities larger than that of their superhalogen building blocks and open the door to the synthesis of powerful oxidizing agents. Recent works have shown that these highly electronegative ions can be used to oxidize water<sup>[22]</sup> as well as increase the oxidation state of metal atoms<sup>[23]</sup>.

Electron counting rules<sup>[24]</sup> have played a significant role in the design and synthesis of many of the recently discovered super- and hyperhalogens. Commonly used rules are the octet

rule, 18-electron rule, and the Wade Mingos rule. The octet rule which requires that for a molecule to be stabilized or an atom to be chemically inert, the outer  $s$  and  $p$  valence electrons must be completely full ( $s^2 p^6$ ). This rule normally applies to light elements with atomic number less than 20. Since halogen atoms have an outer electron configuration of  $s^2 p^5$ , only one electron is needed to complete the shell closing and hence they possess large electron affinities. The 18-electron rule, on the other hand, applies to molecules containing transition metal elements and requires  $s^2$ ,  $p^6$ , and  $d^{10}$  orbitals to be full. As an example, consider  $\text{Au}_{12}\text{Ta}$  [25]. With Au and Ta respectively contributing 1 and 5 valence electrons each,  $\text{Au}_{12}\text{Ta}$  has  $12+5=17$  outer electrons and needs only one electron to satisfy the 18-electron rule. Hence, its electron affinity should be high and this has been confirmed experimentally [25]. It has also been shown that the Wade-Mingos rule which requires  $(n+1)$  pairs of electrons for stable cage-bonding can be used to design superhalogens. An example in this category is borane derivatives. Borane molecules forming polyhedral cages with  $n$  vertices have the formula  $\text{B}_n\text{H}_n^{2-}$ . Thus, if one can replace one B atom by a C atom or add one extra H atom to  $\text{B}_n\text{H}_n^{2-}$ , the corresponding molecules  $\text{CB}_{n-1}\text{H}_n$  or  $\text{B}_n\text{H}_{n+1}$  would require only one electron to satisfy the Wade-Mingos rule. Hence these molecules should possess large electron affinities. Calculations based on density functional theory show this to be true [20] and experimental confirmation of this prediction is awaited.

Until now all of the known superhalogens have been inorganic in nature and organic molecules with electron affinities even approaching those of halogen atoms are not known. The possibility that aromaticity [26,27] rule that accounts for the stability of organic molecules can be used to design superhalogens, has not yet been explored. Aromaticity is a chemical property associated with planar conjugated cyclic systems like Benzene and makes use of free delocalized  $\pi$  electrons to improve its high stability and unusual reactivity patterns. In 1930 Hückel

published his finding on  $\pi$  systems by using molecular orbital theory which is referred to as Hückel molecular orbital theory (HMO). Later in 1931 he generalized<sup>[28]</sup> and extended this theory to benzene and concluded that any conjugated monocyclic polyene that is planar and has  $(4n+2)$   $\pi$  and/or nonbonding electrons, with  $n = 0, 1, 2, \dots$  will exhibit special stability associated with aromaticity. It was not until 1951 when Huckel's  $(4n+2)$   $\pi$  concept was formally clarified by Doering<sup>[29]</sup>. Although Hückel's aromaticity concept has a great impact in organic chemistry, it has been found not to be valid for several compounds like pyrene, coronene etc. which have more than three fused cyclic rings. Recently, the concept of aromaticity has been extended to 3D molecules. In 2000 Hirsch et al<sup>[30]</sup> gave the  $2(N+1)^2$   $\pi$  electron rule for fullerene aromaticity. According to these authors this rule should be applicable to all conjugated  $\pi$  systems including inorganic molecules having symmetrically distributed nuclei over a spherical surface. The aromaticity concept has been further extended to include metals as well through  $\sigma$  and  $\delta$  bond delocalization, though this is still a hotly debated topic<sup>[31]</sup>.

A classic example of an aromatic molecule is benzene,  $C_6H_6$  which has 6  $\pi$  electrons ( $n=1$ ) and a negative electron affinity, namely  $-1.15$  eV<sup>[32]</sup>.  $C_5H_5$ , on the other hand, has 5  $\pi$  electrons and needs one more electron to be aromatic. Consequently, the electron affinity of  $C_5H_5$ , namely,  $+1.79$  eV<sup>[33]</sup> is significantly larger than that of  $C_6H_6$ . However, it is much less than that of any halogen atom. Thus, it is not immediately apparent if molecules designed by following aromaticity concepts can exhibit superhalogen properties. This is because aromatic molecules are usually characterized by covalent bonding where the electrons are localized along the bonds. In a superhalogen, on the other hand, the electrons should be delocalized over a large phase space so that the electron-electron repulsion associated with the added electron is limited.

In this paper we show for the first time that superhalogens can indeed be designed by using Huckel's aromaticity concepts. We show that there are two possible ways of doing this. One is by replacing the H atoms of  $C_5H_5$  with different ligands and the other is by replacing the C atoms of the aromatic core while keeping the  $4n+2$  delocalized  $\pi$  electrons unchanged. The above mentioned two possibilities are described in detail in the following. The main purpose of this paper is to demonstrate that organic molecules can be functionalized to behave as superhalogens. In Section II we describe the theoretical methods used in the search. Results are discussed in Section III and summarized in Section IV.

## II. Theoretical Method

The total energies and equilibrium geometries of the most stable anions and corresponding neutral molecules were calculated using Density Functional Theory (DFT) and B3LYP hybrid functional<sup>[34,35]</sup> for exchange-correlation potential with the 6-311+G(d) basis set embedded in the Gaussian 03 code<sup>[36]</sup>. This has been shown to be effective in similar calculations in the past<sup>[16-21]</sup>. Frequency analysis was also performed at the same level of theory to ensure that there are no imaginary frequencies and the structure belongs to a minimum in the potential energy surface. The Electron Affinity (EA) is calculated as the energy difference between the ground states of the anion and the corresponding neutral. The vertical detachment energy (VDE), on the other hand, is the energy difference between the ground state anion and the corresponding neutral in the anion geometry. The thermal stability was examined by calculating the dissociation energies against different possible fragmentation channels. The charge distribution was analyzed using the Natural Bond Orbitals (NBO) charge on each atom. Nucleus Independent Chemical Shift (NICS) method<sup>[37,38]</sup> was used to establish the aromatic property of

the molecules. The convergence for total energy and force was set at  $1 \times 10^{-6}$  eV and  $1 \times 10^{-2}$  eV/Å, respectively.

### III. Results and Discussions

We begin with the results on  $C_5H_5$  and  $C_6H_6$  primarily to validate our theoretical method and to use them as building blocks in the design of aromatic superhalogens. The equilibrium structures, bond lengths, and calculated electron affinities (EA) are given in Fig. 1 and Table 1 and compared with experiment. The C-C bond lengths are 1.37, 1.44, and 1.48 Å for  $C_5H_5$  and 1.39 Å for  $C_6H_6$ . The C-H bond lengths of  $C_5H_5$  and  $C_6H_6$  are 1.08 Å and 1.09 Å, respectively. These agree well with corresponding experimental values of C-C bonds, namely, 1.34, 1.46, and 1.54 Å and C-H bond, 1.08 Å of  $C_5H_5$ , and C-C bond, 1.40 Å, and C-H bond, 1.09 Å of  $C_6H_6$ . Similarly, the calculated EA of benzene ( $C_6H_6$ ), which is aromatic, is -1.33 eV and is in good agreement with the experimental value of -1.15 eV. However, the fit between the experiment and theory for the negative EAs may be coincidental because of the limits of the computational model in characterizing species with unbound electrons. We have recalculated the EA of benzene at the CCSD level of theory and found it to be -1.83 eV. It is expected that  $C_5H_5$  which needs one extra electron to be aromatic would have a larger electron affinity than that of  $C_6H_6$ . Although this is indeed the case and the calculated EA of  $C_5H_5$  is +1.72 eV (compared to experimental value of +1.79 eV), it is much smaller than that of a halogen atom. At the CCSD level of theory the EA of  $C_5H_5$  is +1.36 eV. Thus, the DFT/B3LYP level of theory overestimates the electron affinity. The question then is: can molecules, using aromaticity rules, be designed such that their EAs are larger than those of halogen atoms? To examine this possibility we adopted a systematic approach.

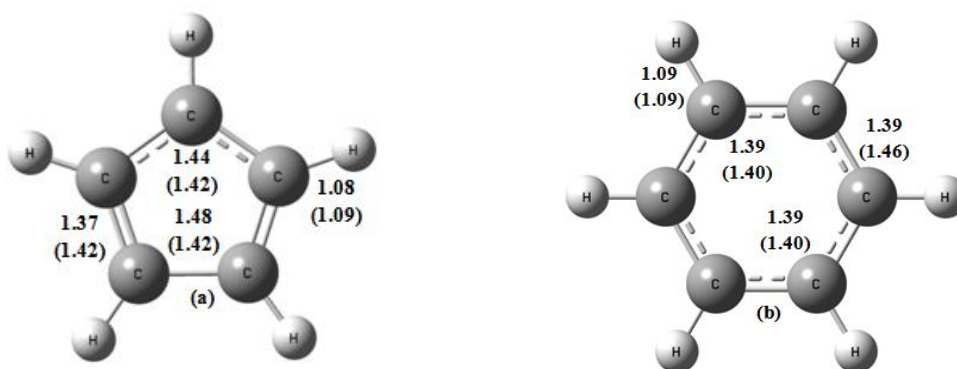


**Fig. 1** Equilibrium geometries of  $C_5H_5$  and  $C_6H_6$ . The bond lengths are given in Å. The bond lengths in brackets are those of the anion.

### A. $C_nX_n$ ( $X= F, CF_3, NCO, CN, BO_2$ ; $n=5, 6$ )

First, we try to design aromatic superhalogens by ligand substitution in  $C_5H_5$ , keeping the aromatic core intact. To do so we replace H in  $C_5H_5$  by different ligands such as F,  $CF_3$ , NCO, CN, and  $BO_2$  since these are far more electronegative than H. For example, the electron affinities of F,  $CF_3$ , NCO, CN,  $BO_2$  are, respectively, 3.40, 1.89, 3.58, 4.07 and 4.35 eV while that of H is only 0.75 eV. The equilibrium geometries of  $C_5X_5$  ( $X= F, CF_3, NCO, CN, BO_2$ ) molecules are given in Fig 2. Note that in the case of  $C_5(CN)_5$  and  $C_5(NCO)_5$ , the C atom on the ring can either bind to the C or N atom of CN and N or O atom of NCO, respectively. In addition, in the case  $C_5(BO_2)_5$  the ligands can dimerize and bind to the C atoms in the ring. Only the lowest energy configurations are given in Fig. 2 and the geometries of the higher energy isomers are given in the supplementary information (SI). Similar calculations were repeated for the benzene,  $C_6H_6$ , where the H atoms were replaced by F, CN,  $BO_2$  ligands. The equilibrium geometries of the  $C_6X_6$  ( $X= F, CN, BO_2$ ) molecules along with their electron affinities are also given in the supporting information (SI).

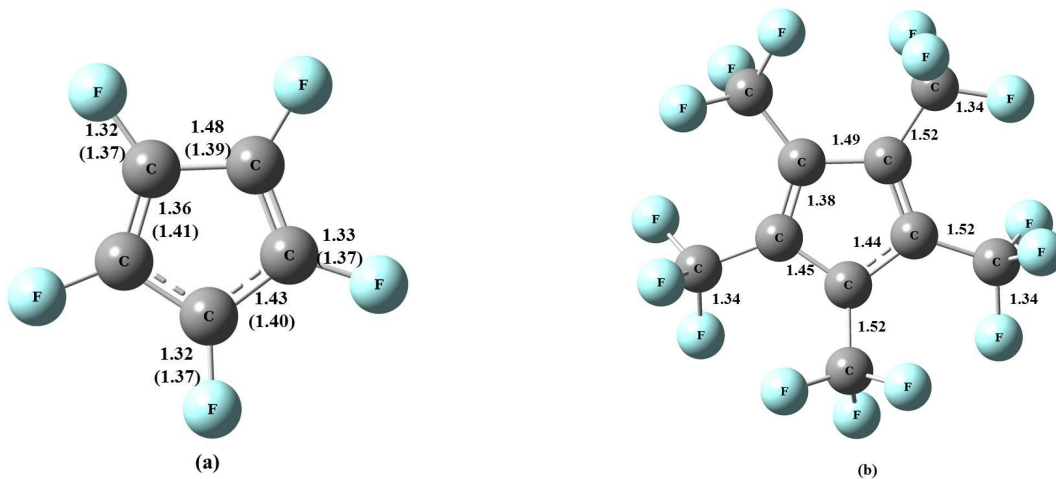
The CF bond length in  $C_5F_5$  is elongated over that of CH bond in  $C_5H_5$  by 0.24 Å. In other molecules in Fig. 2 the bond linking the C atom in the ring to the nearest atom in the ligand



varies between 1.37 Å to 1.52 Å. These bonds are stretched further in the corresponding anions. The C-C bonds in the ring, however, are not affected significantly by the different ligands. The ground state geometry of  $C_5(NCO)_5$  is marked by the C atom in the ring binding to the N atom in the ligand and is 7.80 eV lower than its isomer where the C atom in the ring binds to the O atom in the ligand. In the lowest energy structure of  $C_5(CN)_5$ , the C atoms in the ring bind to the C atoms in the ligands while its isomer with C binding to N lies 5.40 above in energy. The lowest energy structure of  $C_5(BO_2)_5$  departs from the other structures in Fig. 2. Here two of the  $BO_2$  moieties dimerize and bind to four of the carbon atoms in the ring while the fifth carbon atom is bound to the remaining  $BO_2$  ligand. The isomer where each of the C atoms is bound to a single  $BO_2$  unit lies 2.51 eV above the lowest energy structure. This is because the  $BO_2$  moieties gain 1.70 eV of energy by forming a dimer. This, as we will see in the following has important effect on the expected superhalogen property of the  $C_5(BO_2)_5$  molecule.

The EAs of  $C_6F_6$  and  $C_5F_5$  are calculated to be 0.75 eV and 2.68 eV, respectively. Although this is a considerable improvement over the values in  $C_6H_6$  and  $C_5H_5$ , replacing H by F does not lead to a superhalogen. However, the situation changes with different ligands. The EA of  $C_5(CN)_5$  is 5.59 eV, making it a superhalogen. To confirm the accuracy of our method we also calculated the electron affinity of  $C_5(CN)_5$  at the CCSD level of theory. The corresponding value, namely 5.30 eV, is 0.3 eV less than that of the value at the CCSD level of theory. This is consistent with previous results [G. Chen, Q. Sun, Q. Wang, Y. Kawazoe, and P. Jena, *J. Chem. Phys.* **132**, 194306 (2010)] that the electron affinities calculated at the DFT level of theory is usually accurate within about 0.2 eV. The EA of  $C_5(NCO)_5$  and  $C_5(BO_2)_5$  are 3.28, and 3.45 eV, respectively. Although these are significantly enhanced over that of  $C_5F_5$ ,  $C_5(NCO)_5$  and  $C_5(BO_2)_5$  do not belong to the superhalogen category. The reason for  $C_5(BO_2)_5$  not becoming a

superhalogen is due to the preference of  $\text{BO}_2$  moieties to dimerize. Had that not been the case and each of the C atoms in the ring would have bound to individual  $\text{BO}_2$  moieties, the electron affinity of such a complex would have been 4.25 eV, making it a superhalogen. The probable reason for  $\text{C}_5\text{F}_5$  and  $\text{C}_5(\text{NCO})_5$  not becoming a superhalogen is that the  $\pi$  donating nature of F and NCO works against it. The same conclusion also holds for  $\text{BO}_2$ . CN as a ligand works



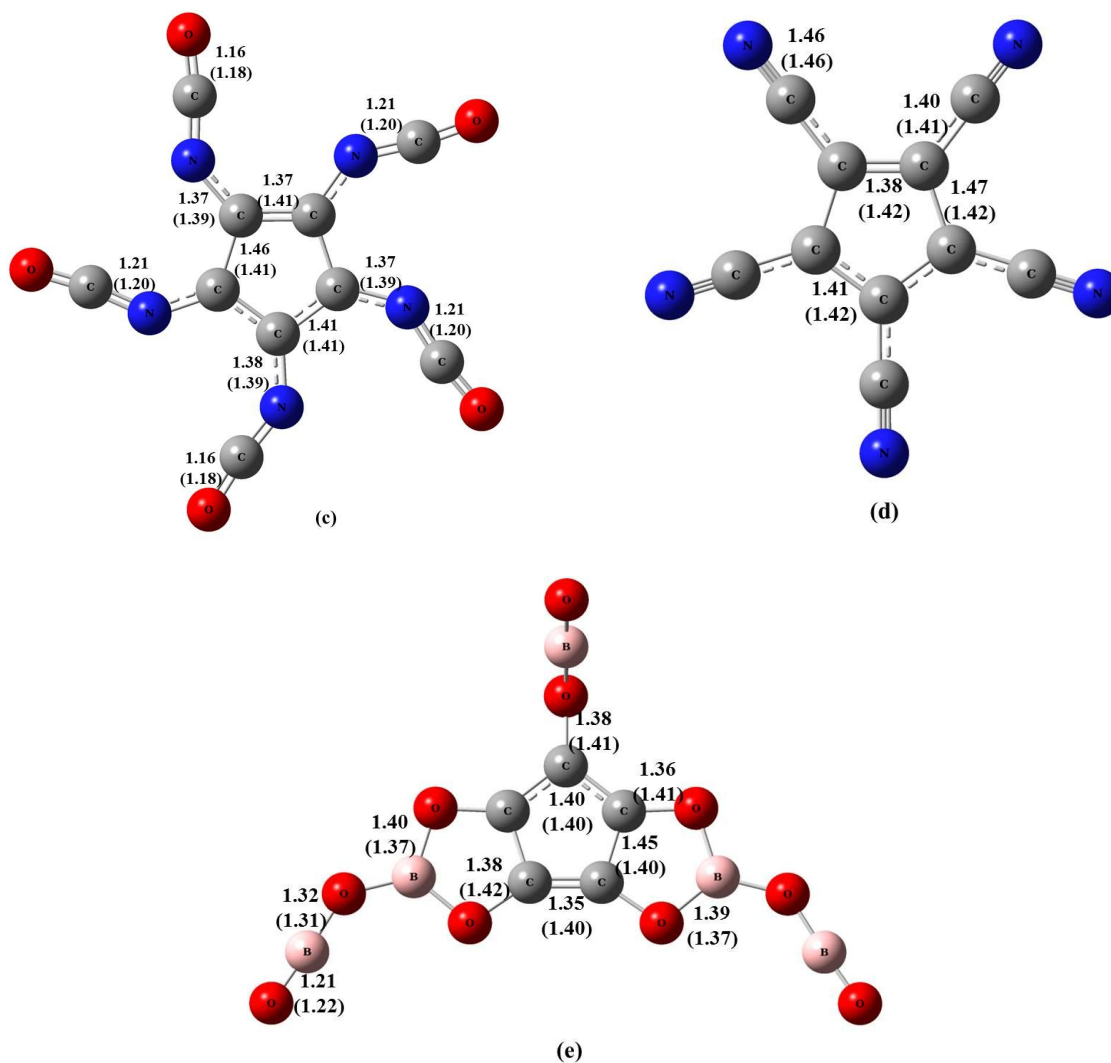


**Fig. 2** Equilibrium geometries of  $C_5X_5$  ( $X = F, CF_3, NCO, CN, BO_2$ ). The bond lengths are given in Å. The bond lengths in brackets are those of the anions.

better for making a superhalogen because of its dual nature. CN is not only a strong electron withdrawing group but also it has relatively high electron affinity. So it is clear that electron withdrawing effect of ligand drives the formation of superhalogen compounds.

To check this idea further we considered  $CF_3$  ligand which belongs to an electron withdrawing group having low EA value (1.89 eV). To calculate EA of  $C_5(CF_3)_5$  molecules we tried to optimize both the neutral and the anion geometry. While we were successful in optimizing the neutral geometry, the optimization of its anion geometry led to problems. The

imaginary negative frequencies were associated with the rotation of the  $\text{CF}_3$  unit in  $\text{C}_5(\text{CF}_3)_5$ . Therefore, we calculated the vertical attachment energy (VAE) which is the energy gained by attaching an electron to the neutral structure without optimizing its geometry. In this sense the VAE is lower bound to the EA. The calculated VAE value of  $\text{C}_5(\text{CF}_3)_5$ , namely 4.58 eV, suggests that  $\text{C}_5(\text{CF}_3)_5$  indeed is a superhalogen molecule, owing to the electron withdrawing property of  $\text{CF}_3$  ligand. In fact we compared the VAE of  $\text{C}_5(\text{CF}_3)_5$  with that of  $\text{C}_5(\text{CN})_5$ . We found that the VAE of  $\text{C}_5(\text{CN})_5$  is 5.46 eV which is smaller than its EA, namely 5.59 eV.

### **B. $\text{C}_{n-m}\text{H}_{n-m}\text{N}_m$ ( $n=5, 6$ ; $m=0-3$ )**

We then considered the second possibility, replacing a CH group with an N atom. Note that this replacement leaves the total number of valence electrons unchanged as both CH and N are isoelectronic. Hence, aromatic properties would not be affected by this substitution. However, the electron affinities of CH and N are, respectively, 0.077 eV and 0.073 eV<sup>[39]</sup>. On this basis one might expect that successive replacement of CH with N in  $\text{C}_6\text{H}_6$  and  $\text{C}_5\text{H}_5$  may not lead to moieties with larger electron affinities. However, a previous experimental study had shown

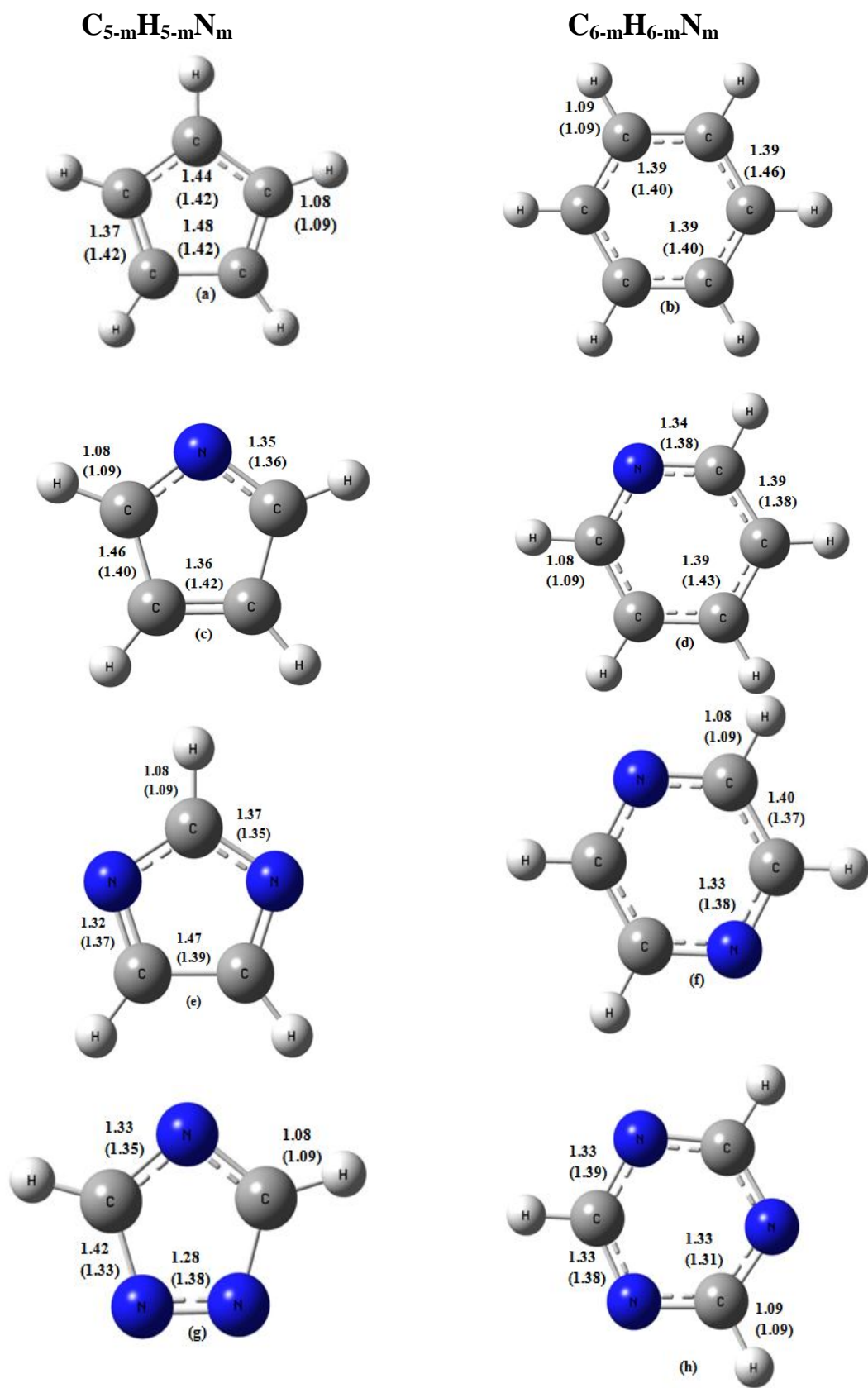


**Fig. 3** Equilibrium geometries of  $C_{n-m}H_{n-m}N_m$  ( $n=5, 6, m=0-3$ ). The bond lengths are given in Å. The bond lengths in brackets are those of the anion.

that the EA of C<sub>5</sub>H<sub>5</sub>N (pyridine) is -0.62 eV<sup>[32]</sup> which is much more positive than the EA of isoelectronic C<sub>6</sub>H<sub>6</sub>, namely, -1.15 eV. To study the effect of successive replacement of CH groups with N atoms we calculated the structure and total energies of C<sub>n-m</sub>H<sub>n-m</sub>N<sub>m</sub> (n=5, 6; m=1-3) systematically. In Fig. 3 we present the geometries of these molecules. The corresponding EAs are given in Table 1. The calculated EA of pyridine is -0.74 eV which is in good agreement with the experimental value (-0.62 eV) given in Table 1. We note that the EA increases steadily with increasing number of N substitutions. The calculated EA of pyrazine and s-triazine where the N atoms are substituted at the 1, 4 and 1, 3, 5 sites are -0.04 eV and +0.008, respectively. These also agree well (within the accuracy of the DFT methods) with the corresponding experimental values of +0.065 eV and +0.124 eV<sup>[32]</sup>. We note that none of these molecules mimic halogens, let alone superhalogens. No experimental values of EA of C<sub>5-m</sub>H<sub>5-m</sub>N<sub>m</sub> (m > 0) are available. However, our computed values show that the EAs continue to increase and reach a value of 3.46 eV for C<sub>2</sub>H<sub>2</sub>N<sub>3</sub>, making this molecule a pseudo-halogen. This shows that it is unlikely that modification of the core of C<sub>5</sub>H<sub>5</sub> could render it superhalogen properties.

Table 1: Electron Affinities (in eV) of C<sub>n-m</sub>H<sub>n-m</sub>N<sub>m</sub> (n=5, 6, m=0-3)

m, # N replaced	C <sub>6-m</sub> H <sub>6-m</sub> N <sub>m</sub>		C <sub>5-m</sub> H <sub>5-m</sub> N <sub>m</sub>	
	Theory	Experiment	Theory	Experiment
0	-1.33(-1.83)*	-1.15	1.73(1.36)*	1.79
1	-0.74	-0.62	2.08	
2	-0.04	0.065	2.58	
3	0.008	0.124	3.46	

\* Value given in parenthesis is the data calculated at CCSD/6-311+G(d)

### C. $C_{13-m}H_{9-m}N_m$ ( $m=0-3, 9$ )

To search for other routes that can enable organic molecules to have electron affinities higher than that of  $C_2H_2N_3$ , we drew inspiration from an earlier work by Gonzales *et al*<sup>[40]</sup> where the authors studied a series of molecules by fusing a five-membered ring ( $C_5H_6$ ) with increasing numbers of six-membered rings. Note that there are two ways to fuse these rings; the five-membered ring may be fused either at the end of the chain or in the middle. The first arrangement with one five-membered ring sandwiched between two six-membered rings is known as fluorene while the latter with a five-membered ring attached at the end of the two fused six-membered rings yields a molecule known as benzo[*f*]indene. At the B3LYP level of theory with the 6-311++G\* basis sets the calculated EAs<sup>[40]</sup> of the radicals formed by cleavage of a C-H bond in the 5-membered ring, i.e., cyclopentadienyl ( $C_5H_6$ ), indenyl ( $C_9H_8$ ), and fluorenyl ( $C_{13}H_{10}$ ), were found to be -0.66 eV, -0.55 eV, and -0.27 eV, respectively. Note that the parent molecules have saturated carbons in the 5-membered ring and the C-H cleavage at this carbon is needed to give a fully delocalized  $\pi$ -system. Addition of an electron gives a closed-shell anion with an aromatic electron count in the  $\pi$ -system. The trend clearly shows that by increasing the length of the organic framework the electron affinity can steadily increase. This is consistent with the expectation that electron affinities tend to increase as electrons are more delocalized.

Since replacement of CH with N or H with F as well as incorporating benzoannulated cyclopentadienyl units tend to increase electron affinities, we considered the base structure of the fluorenyl radical ( $C_{13}H_9$ ) as a starting point in our search for aromatic superhalogens. Note that  $C_{13}H_9^-$  satisfies the aromaticity rules. Similar to what was done for  $C_nH_n$  ( $n=5, 6$ ) we first replaced H with F. This did not increase EAs significantly. These results are given in the

supplementary information (SI). Next we replaced up to three CH groups with three N atoms successively by considering both the fluorene and benz[*f*]indene frameworks. In the following we present our results.

(i) *Equilibrium Geometries of the negative ions:*

In photoelectron spectroscopy experiments (PES) the starting point is the negative ion. Therefore, we first present the optimized geometries of the most stable isomer of the anionic  $C_{13-m}H_{9-m}N_m$  ( $m=0-3$ ) molecules in Fig. 4(a-e). The ground state of the anionic  $C_{13}H_9$  molecule in Fig. 4(a) has the five-membered ring sandwiched between the two six-membered rings (fluorene structure). The higher energy isomer has the benz[*f*]indene structure and lies only 0.29 eV above the ground state (see Fig. 5(a)). These results agree with earlier studies of Gonzales *et al*<sup>[40]</sup>.

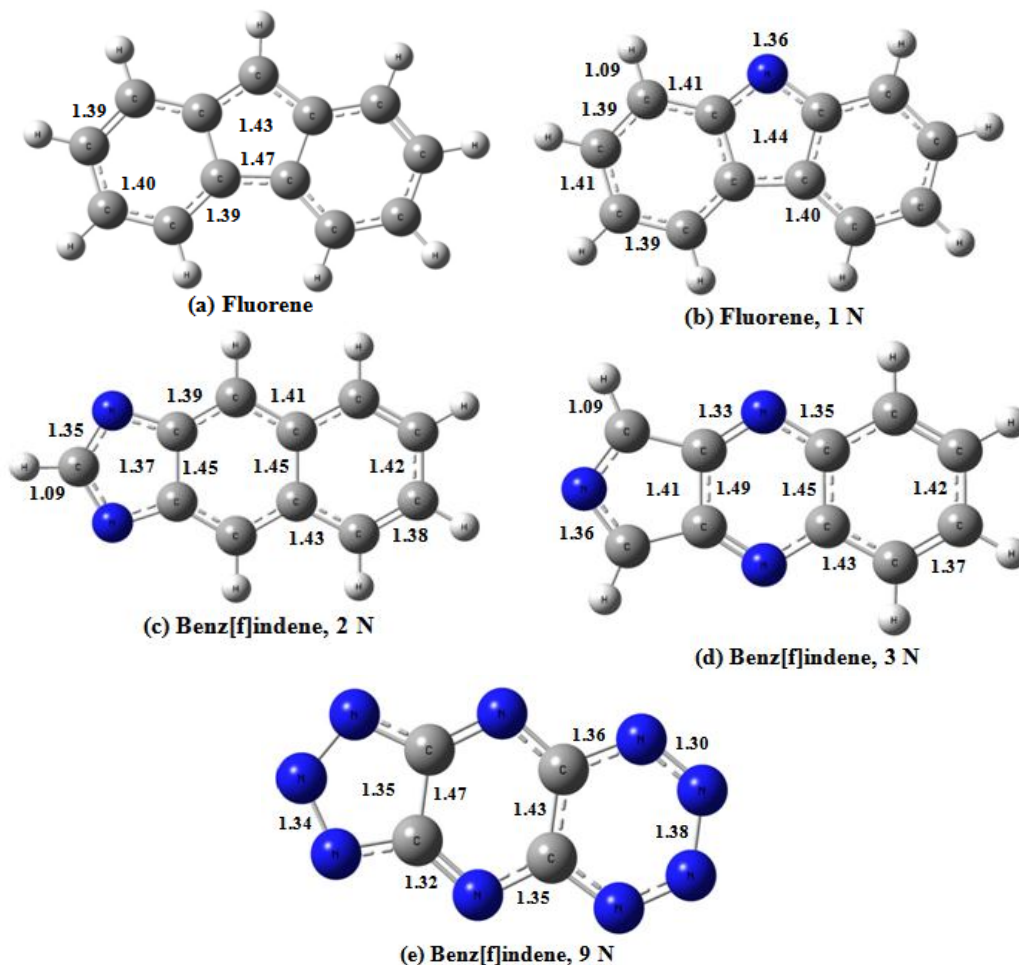


**Fig. 4:** Equilibrium geometries of anionic  $C_{13-m}H_{9-m}N_m$  ( $m=0-3, 9$ ) molecules. Bond lengths are in Å.



When one of the CH groups is replaced by an N atom, the preferred geometry of the anionic  $C_{12}H_8N$  continues to have the fluorene structure. The N atom occupies the 9-position (Fig. 4(b)). The bond lengths are symmetric from left to right and vary from 1.39 Å to 1.41 Å. The nitrogen bonds shorten to 1.36 Å. In Fig. 5(b) we show the geometry of the next higher energy isomer lying 0.65 eV above the ground state. It has the benz[f]indene structure where the N atom occupies the end site of the five-membered ring.

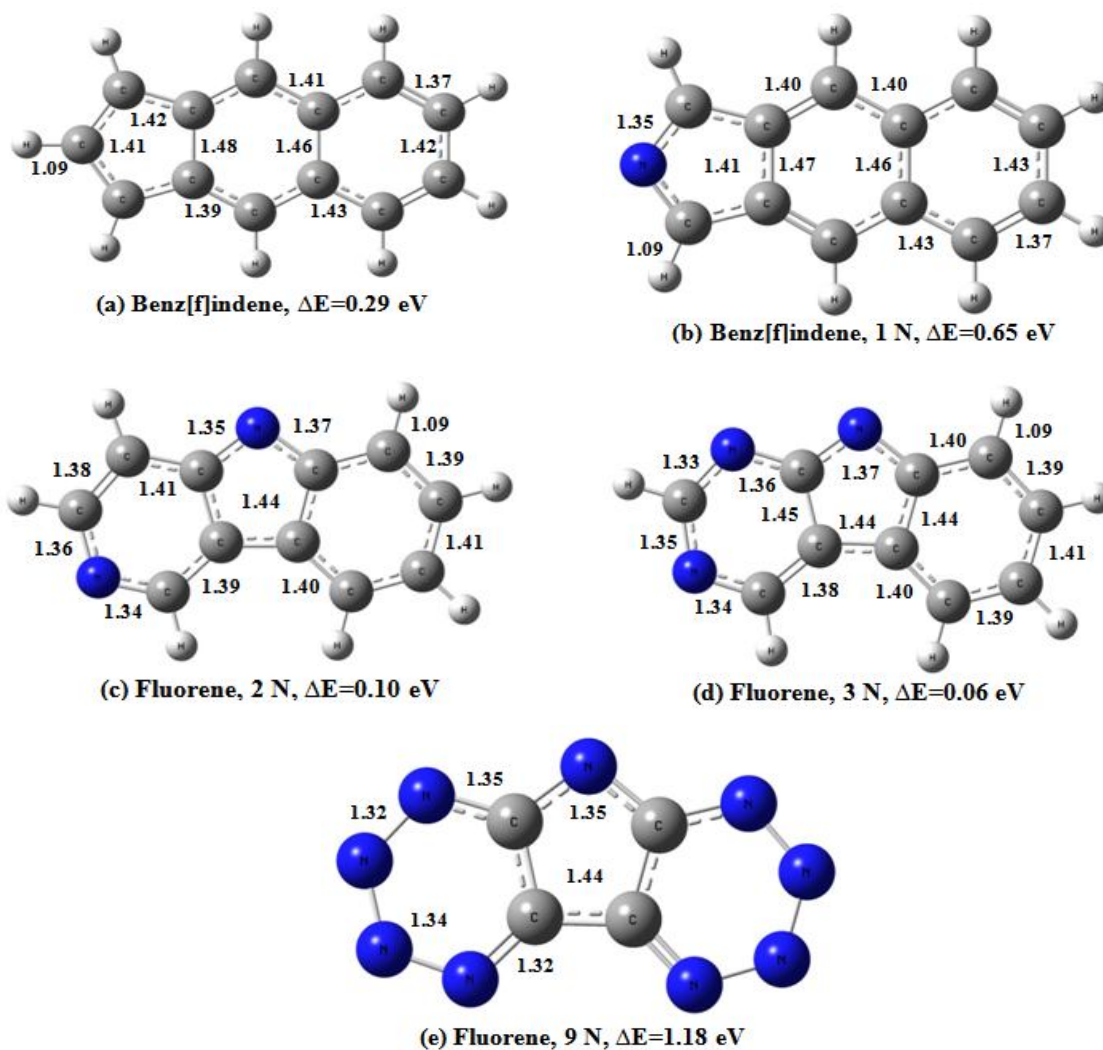


**Fig. 5:** Geometries of next higher energy isomers of anionic  $C_{13-m}H_{9-m}N_m$  ( $m=0-3, 9$ ) molecules. Bond lengths are in Å.

Next we discuss the replacement of two CH groups with two N atoms. All possible sites for the N atoms were tried and the preferred structure of the anionic  $C_{11}H_7N_2$  molecule is shown in Fig. 4(c). Unlike the  $C_{12}H_8N$  structure, the  $C_{11}H_7N_2$  anion has the benz[*f*]indene structure with the N atoms occupying next nearest neighbor sites in the five-membered ring. The four nitrogen bonds range in length from 1.34 Å to 1.37 Å, while the benzene ring's bond lengths stay unchanged. The bonds in the five-membered ring also increase, but only slightly to 1.45 Å. Preferred locations of N atoms in the next higher energy isomer given in Fig. 5(c) are different as is the structure. The anion assumes the fluorene structure and lies 0.1 eV above the ground state. One N atom occupies the 9-position of fluorene while the second occupies the farthest site in the six-membered ring. We note that even though the two isomers are rather close in energy, a substantial energy barrier will be involved in going from the benz[*f*]indene structure to the fluorene structure. Thus, if the molecules are born as anions, it is the VDE of the benz[*f*]indene structure that the PES experiment will measure.

The preferred geometry of the  $C_{10}H_6N_3$  anion is shown in Fig. 4(d). It has again the benz[*f*]indene structure with one of the N atoms occupying the apex site of the five-membered ring while the other two occupy opposite sites in the central six-membered ring. The only change that occurs in the bonds is that those adjacent to the third nitrogen shorten to 1.33 Å and 1.36 Å leaving the far side of the structure unaffected. The corresponding higher energy isomer is shown in Fig. 5(d). Here the anion has the fluorene geometry lying only 0.06 eV above the ground state. One N atom occupies the apex site of the five-membered ring while the other two occupy next nearest neighbor sites of the six-membered ring. Both isomers can be considered to be energetically degenerate and in a PES experiment both are likely to be present. As a general

remark, we note that by the time two CH groups are replaced by two N atoms, the anions assume benz[*f*]indene form.

For reasons that will be clear in the following sub-section we next considered structures where all the CH groups were replaced with N atoms. The preferred geometry of the C<sub>4</sub>N<sub>9</sub> anion is shown in Fig. 4(e). It assumes the benz[*f*]indene structure. The corresponding geometry of the higher energy isomer is given in Fig. 5(e). The fluorene structure of the anion is 1.18 eV less stable than the benz[*f*]indene form.

**(ii) Vertical Detachment Energies:**

The vertical detachment energies (VDE) of C<sub>13-m</sub>H<sub>9-m</sub>N<sub>m</sub> (m=0-3, 9) molecules are given in Table 2. The VDE of C<sub>13</sub>H<sub>9</sub> is 1.82 eV. It increases by 0.69 eV when only one CH group is replaced by N, namely the VDE of C<sub>12</sub>H<sub>8</sub>N is 2.51 eV. The VDEs of C<sub>11</sub>H<sub>7</sub>N<sub>2</sub> and C<sub>10</sub>H<sub>6</sub>N<sub>3</sub> are, respectively, 2.94 eV and 3.57 eV. Although the VDEs increase with the successive replacement of CH groups with N atoms, C<sub>11</sub>H<sub>7</sub>N<sub>2</sub> and C<sub>10</sub>H<sub>6</sub>N<sub>3</sub> are still far from being a superhalogen. At best, C<sub>10</sub>H<sub>6</sub>N<sub>3</sub> can be termed as a pseudohalogen as its electron affinity approaches that of Cl. Note that while none of these molecules qualify as superhalogens, the VDEs steadily rise with the replacement of CH groups with isoelectronic N. Consequently, we tried the ultimate structure where all the CH groups are replaced with N atoms. This leads to the molecule with formula C<sub>4</sub>N<sub>9</sub> which has a VDE of 5.28 eV, clearly making it a superhalogen.

**(iii) Ground State Geometries of Neutral Molecules, Electron Affinities and Adiabatic Detachment Energies:**

In a PES experiment the first peak in the spectrum corresponds to the vertical detachment energy (VDE) which signifies the least energy needed to remove the extra electron from the anion without changing its structure.

Table 2: VDE, EA, and ADE (in eV) of  $C_{13-m}H_{9-m}N_m$  for  $m=0-3, 9$ .

# CH groups replaced by N	VDE	EA	ADE
0	1.82	1.74	1.74
1	2.51	2.41	2.43
2	2.94	2.77	2.88
3	3.57	3.10	3.32
9	5.28	4.58	4.58

However, following the electron detachment the neutral cluster will relax. In most cases the neutral cluster will reach its ground state. However, if the geometries of the ground states of the anion and its corresponding neutral are very different and are separated by a large energy barrier, the neutral cluster, following electron detachment, will relax to its nearest potential energy minimum. The difference between the total energy of the anion and its structurally similar neutral is known as adiabatic detachment energy (ADE) while that between the ground states of the anion and its neutral is referred to as the electron affinity (EA). In most cases the ADE and EA values are rather close, although exceptions do exist (see *SI*). To see how different are the lowest energy geometries of the neutral  $C_{13-m}H_{9-m}N_m$  ( $m=0-3, 9$ ) molecules from their anions, we have optimized their structures. The results are presented in Fig. 6(a-e). The geometries of the next higher energy isomers are given in Fig. 7. The ground state of neutral  $C_{13}H_9$  has the fluorene

structure, same as that of the anion. The higher energy isomer with the benz[*f*]indene structure lies 0.23 eV above the fluorene structure.

Although neutral  $C_{12}H_8N$  has the same fluorene structure as its anion, the placement of the N atom is different. In the neutral structure, nitrogen occupies the base of the benzene ring adjacent to the five-membered ring. As in the anion, the nitrogen bonds are shortened to 1.34 and 1.32 Å. The rest of the benzene bonds are 1.40 Å, with the exception of the bonds symmetric with the nitrogen bonds which are 1.38 Å. The bonds of the five-membered ring are 1.43 Å for four sides

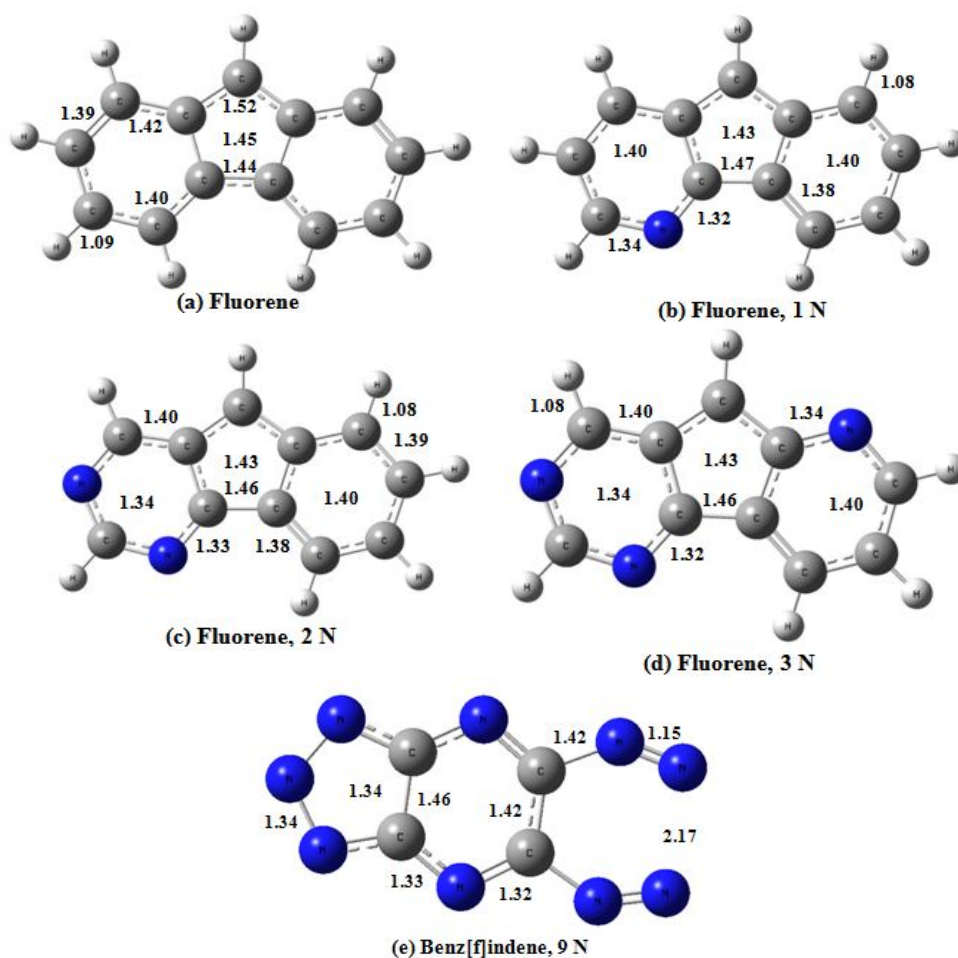


**Fig. 6:** Ground state geometries of neutral  $C_{13-m}H_{9-m}N_m$  ( $m=0-3, 9$ ) molecules. Bond lengths are in Å.

and the base is 1.47 Å. The geometries of neutral  $C_{11}H_7N_2$  and  $C_{10}H_6N_3$  have fluorene structure while their anions have the benz[*f*]indene structure.

The nitrogen atoms occupy next nearest neighbor sites of a six-membered ring. In  $C_{10}H_6N_3$  the third nitrogen prefers the second six-membered ring and occupies the CH site closest to the five-membered ring. Here, the only change to the bond lengths is that the bonds associated with the third nitrogen atom reduce to 1.34 Å. The ground state of neutral  $C_4N_9$  has the same benz[*f*]indene structure as its anion. The EAs and ADEs of  $C_{13-m}H_{9-m}N_m$  ( $m=0-3, 9$ ) molecules are listed in Table 2. Note that in spite of the large differences in the geometries of the anion and neutral, the EA values are not very different from those of the VDEs. This is because changing the location of N atoms does not affect the energies significantly, although they will face significant energy barriers to do so.

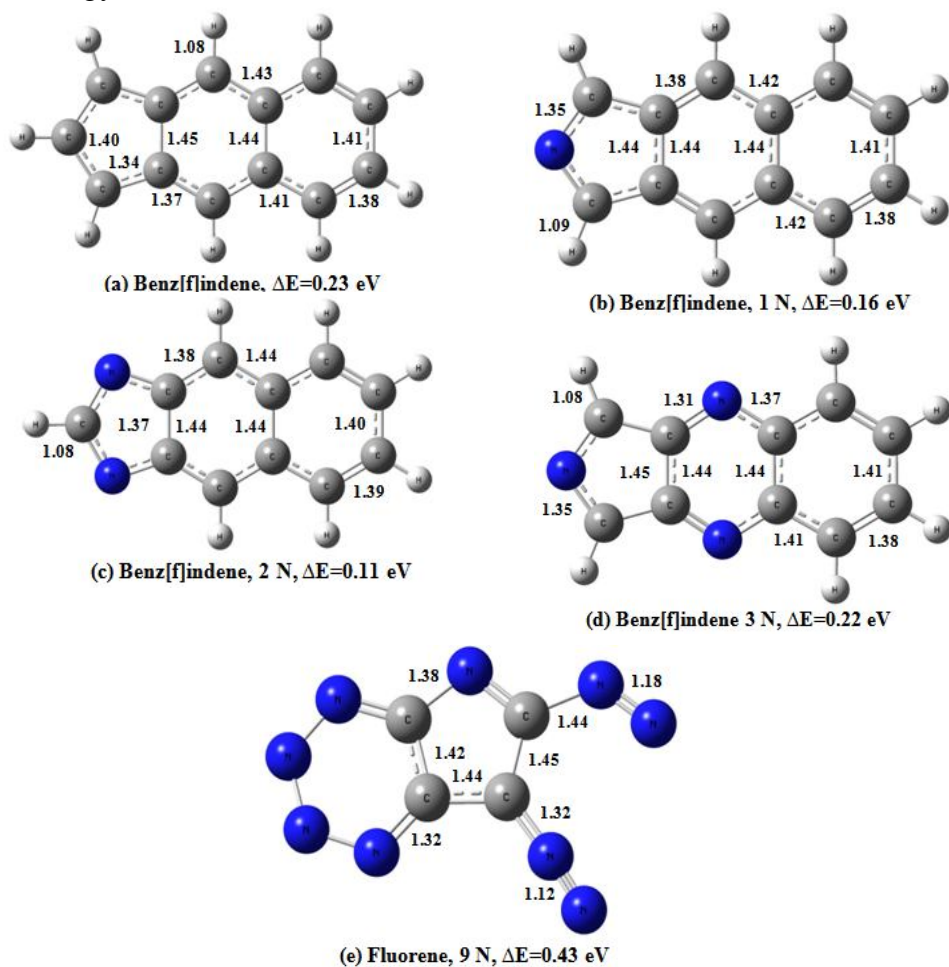


**Fig. 7:** Geometries of next higher energy isomers of neutral  $C_{13-m}H_{9-m}N_m$  ( $m=0-3, 9$ ) molecules. Bond lengths are in Å.

(iv) **Thermal Stability:**

We note from the above that  $C_4N_9$  is a superhalogen and is vibrationally stable since all frequencies are positive. But, is it thermally stable? To examine its thermodynamic stability we calculated the dissociation energies of neutral  $C_4N_9$  against possible fragmentation pathways. First, we considered fragmentation into  $C_4N_7+N_2$  and  $C_4N_5+2N_2$ . The first channel is endothermic by 1.11 eV while the second one is exothermic by 0.47 eV [see Fig. 8(a)]. The fragmentation of  $C_4N_9$  where the  $N_2$  molecule is removed from the five-membered ring is endothermic by 0.74 eV. To see if a superhalogen can be created that is *thermally stable* we considered  $C_6N_7H_2$  where the two N atoms in the  $C_4N_9$  molecule are replaced by two CH groups [see Fig. 8(b)]. This structure is *stable* against the fragmentation pathway where  $N_2$  breaks away from the five-membered ring. And, most importantly, it is a superhalogen with vertical detachment energy of 4.66 eV.

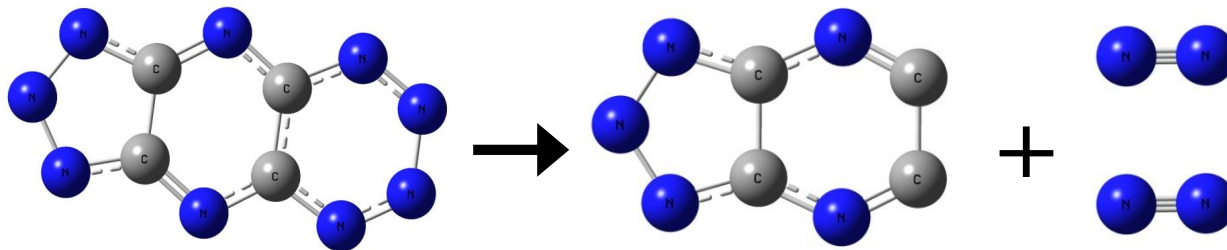


**Fig. 8(a):** Fragmentation reaction pathway

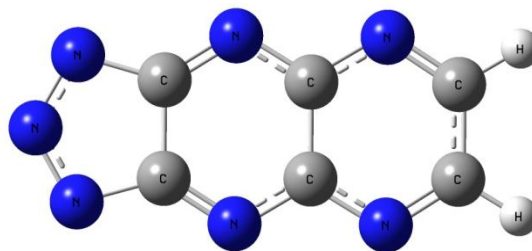


**Fig. 8(b):**  $C_6N_7H_2$ , thermally stable

## D. Beyond tricyclic poly aromatic hydrocarbons (PAH)

We note that Gonzales *et al*<sup>[40]</sup> had shown that by increasing the number of benzene rings the EA of a molecule could be increased. To see if replacement of CH groups with N and further addition of benzene rings can continue to yield moieties with higher electron affinities, we studied the structure and properties by successively adding up to six benzene rings to a five-membered ring. The corresponding geometries of the anions are given in Fig. 9. The resulting EAs and VDEs are illustrated in Fig. 10, and the values are presented in Table 3. Note that the EAs and VDEs continue to rise and reach a value of 5.12 and 5.33 eV, respectively. From the NBO charge distributions we found the additional charge to be mostly associated with the

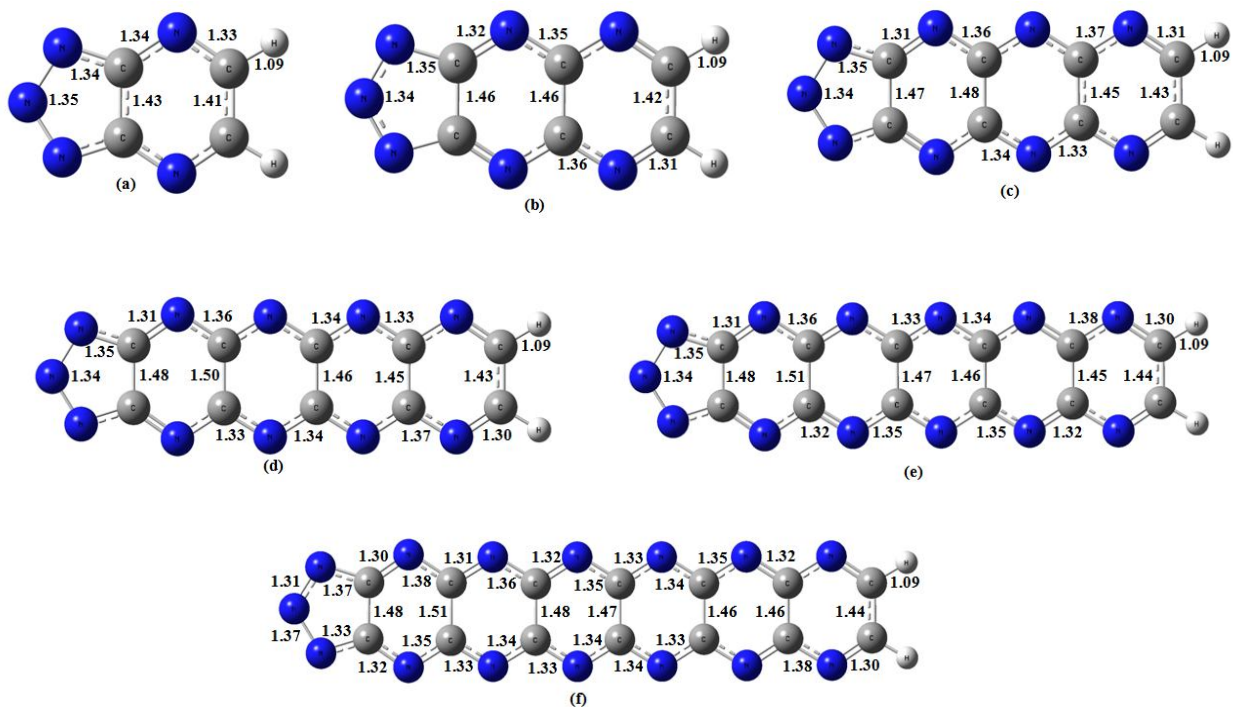


**Fig. 9:** Ground state geometries of anionic PAH molecules. Bond lengths are in Å.

nitrogen located at sites in the five-membered ring. The nitrogen atoms located in the six-



membered rings have a diminishing charge with increasing distance from the five-membered ring.

Table 3: Electron Affinities (EA) and Vertical Detachment Energies (VDE) of poly aromatic hydrocarbons

	EA	VDE
1 Benzene	4.03 eV	4.36 eV
2 Benzene	4.36 eV	4.66 eV
3 Benzene	4.62 eV	4.95 eV
4 Benzene	4.82 eV	5.09 eV
5 Benzene	4.98 eV	5.23 eV
6 Benzene	5.12 eV	5.33 eV

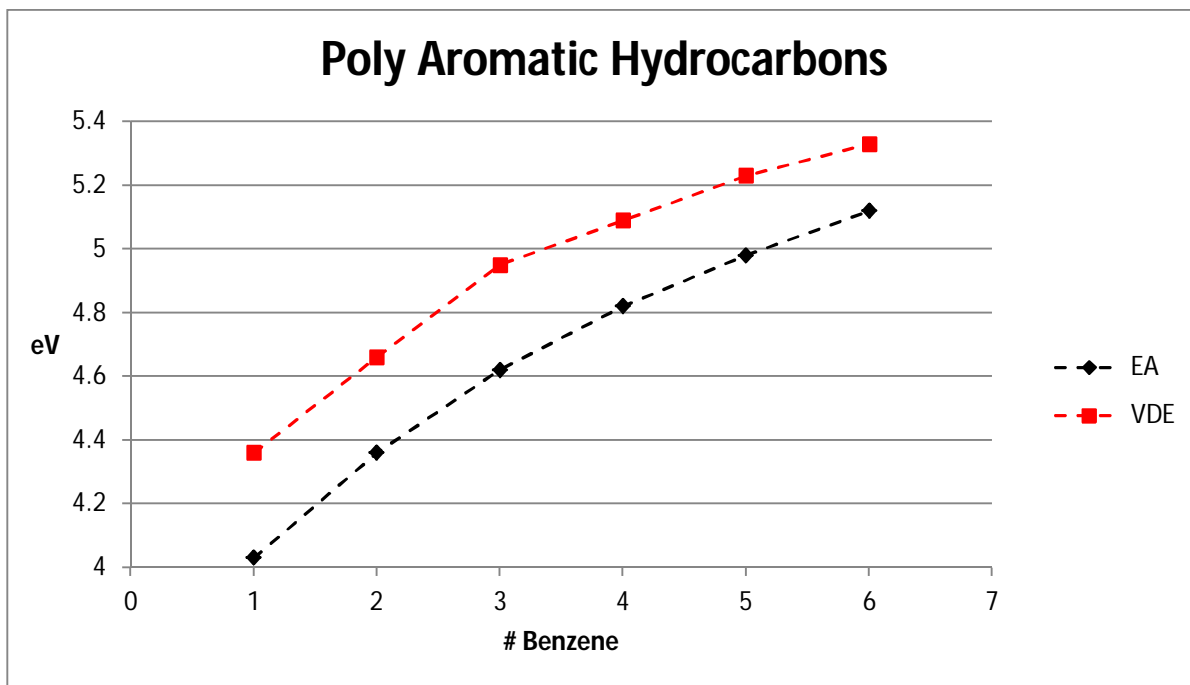


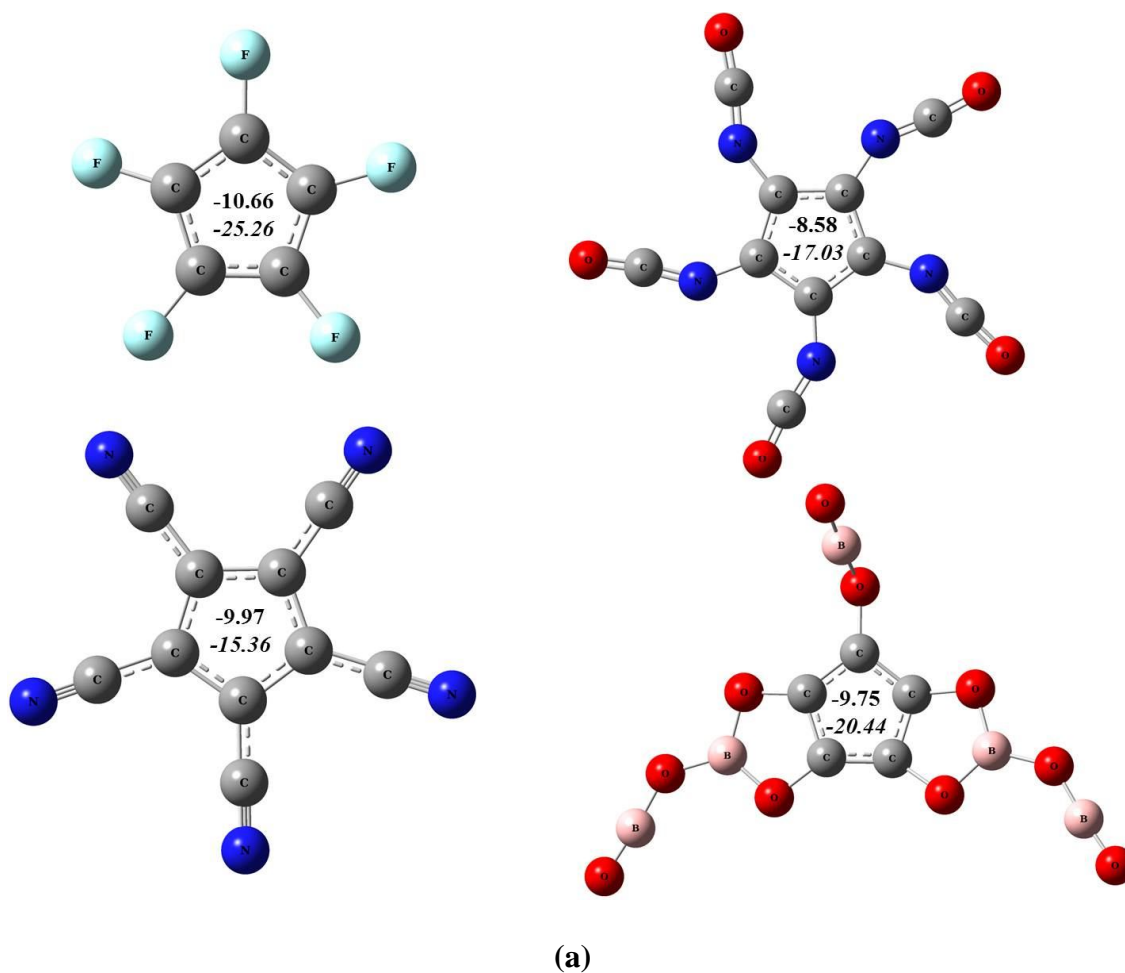
Fig. 10: EA and VDE of larger nitrogen replaced PAH molecules

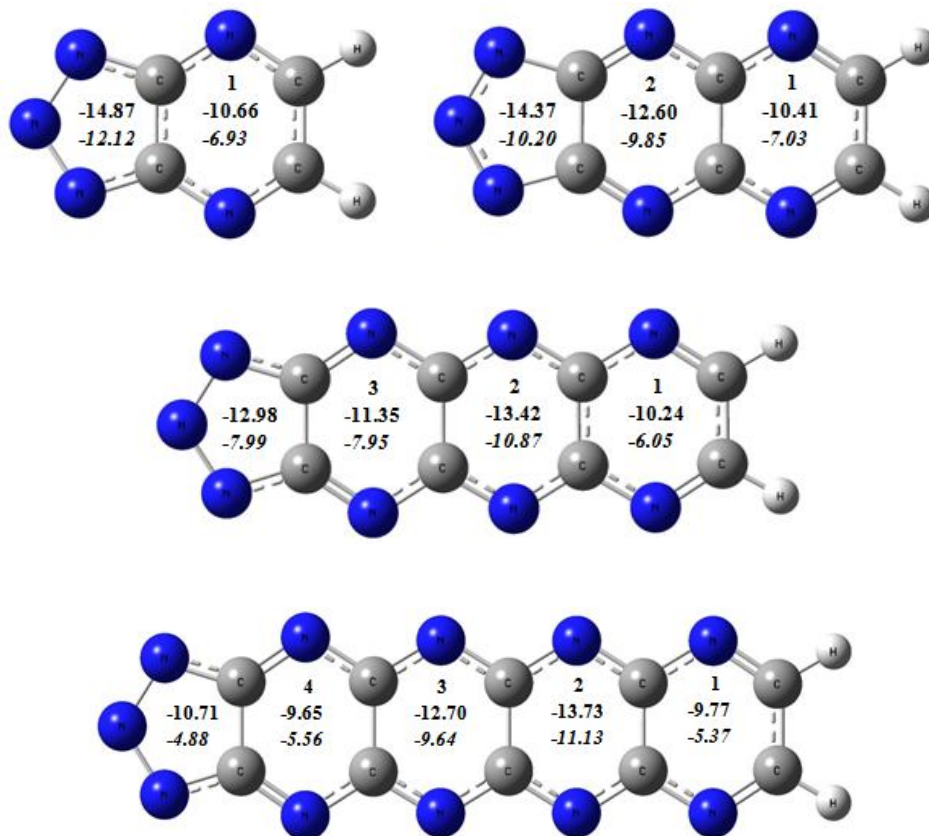
## E. Aromaticity

Aromaticity can be considered as an indicator of cyclic delocalization of electrons moving freely around the ring. There are different methods available in the literature to predict the aromaticity of a molecule. Some of these are diamagnetic susceptibility exaltation, electron localization function (ELF), harmonic oscillator model of aromaticity (HOMA), nucleus-independent chemical shift (NICS), etc. Here we have adopted the NICS method developed by Schleyer and coworkers<sup>[27, 37, 38]</sup>. NICS is defined as the *negative* of the absolute magnetic shielding computed at the un-weighted geometric center of an aromatic or antiaromatic ring [NICS(0)], or 1 Å above the ring [NICS(1)]. Significantly negative NICS values indicate the presence of a diatropic ring current and, therefore, aromaticity in the system. To confirm the aromaticity of these molecules we calculated the chemical shift<sup>[37,38]</sup> at the center of the ring and 1 Å above it for C<sub>5</sub>X<sub>5</sub> (X= F, NCO, CN, BO<sub>2</sub>) as well as the first four molecules in Fig. 9. We also studied how these change with ligand and size. We recognize that the increase in the NICS value above the ring is due to the existence of  $\pi$  electrons. Fig. 11 shows the structures with their calculated NICS values (in ppm). The NICS value 1 Å above the plane is listed first, and the NICS value at the center is listed second in *italics*.

We have found that for all the cases of C<sub>5</sub>X<sub>5</sub> (X= F, NCO, CN, BO<sub>2</sub>) (see Fig. 11(a)) the molecules are aromatic due to their negative NICS values. In fact the aromaticity increases in comparison to that of the cyclopentadienyl anion. We also found that with an increase in aromaticity, the EA also increases. For the second sets of molecule (Fig 11 (b)) the cyclopentadienyl anion starts out with the highest NICS value for both in the plane and above it. As more benzene rings are added, the aromaticity in the ring decreases. The NICS value of the benzene ring at the end of the chain (marked “1”) also decreases with increasing chain length.

However, the aromaticity of the inner benzene rings marked “2-4” increases with chain length, with each subsequent ring starting with a smaller NICS value than the ones before. The lowest value is -4.88 ppm which is significantly lower than that of benzene’s NICS, namely -9.70 ppm. The decrease in the NICS value of the cyclopentadienyl anions as well as the end benzene ring means that the  $\pi$  electrons are less delocalized. This is compensated by the increase in the chemical shift of the inner benzene rings which suggests that the electrons in these rings are more delocalized. It is because of these competing effects that the increase in electron affinities with successive addition of benzene rings slows and tends to saturate.





(b)

**Fig. 11:** NICS values (in ppm) for  $C_5X_5$  ( $X = F, NCO, CN, BO_2$ ) and first four PAH molecules of Fig. 9. First value is 1 Å above plane, second value, in italics, is in the plane.

#### IV. Conclusions

We recall that electron counting rules have played a major role in the design and synthesis of a large number of superhalogens over the past 30 years and these superhalogens have the potential to lead to new salts as well as to new chemistry. Among these rules, the octet rule applies to light atoms with atomic number less than 20, the 18-electron rule applies to molecules containing transition metal atoms, and the Wade-Mingos rule applies to borane-derivatives. It has been shown that molecules that require only one extra electron to satisfy the above rules can have large electron affinities. However, no organic molecule that satisfies the aromaticity rule

when one extra electron is added has been shown to mimic a halogen, let alone behaving as a superhalogen. Using density functional theory and hybrid functional (B3LYP) for exchange-correlation potential we have studied the geometries, electronic structure, thermal stability, vertical detachment energies, electron affinities, adiabatic detachment energies, and aromatic properties of a number of molecules formed by either by tailoring the ligands of cyclopentadienyl or by multiple benzo-annulations of cyclopentadienyl in conjunction with the substitution of CH groups with isoelectronic N atoms.

We demonstrate that these methods allows the creation of aromatic superhalogens with electron affinities as high as 5.12-5.59 eV. These molecules consist of the formula  $C_5X_5$  ( $X=CN$ ,  $CF_3$ ) and  $C_{4+2n}N_{5+2n}H_2$  ( $n = 0 - 5$ ). Both methods mentioned above show promise in creating superhalogens; the first method leads to higher EA, while the second can be tailored to yield electron affinity of almost any desired value by altering chain length and N substitution sites. Thermal stability of these new species has been further examined by calculating the energies necessary to fragment these molecules using pre-determined fragmentation pathways. The Nucleus Independent Chemical Shift (NICS) method was used to confirm the aromaticity of these anions. Our study provides new possibilities for the synthesis of organic superhalogens as wells as new insight into the mechanisms through which they can be synthesized. We hope that our study will stimulate experimental efforts.

**Acknowledgement:** This work was supported in part by the U. S. Department of Energy, Office of Basic Energy Sciences, Division of Materials Sciences and Engineering under Award # DE-FG02-96ER45579. Resources of the National Energy Research Scientific Computing Center supported by the Office of Science of the U.S. Department of Energy under Contract No. DE-

AC02-05CH11231 is also acknowledged. BZC thanks Ms. Swayamprabha Behera for numerous discussions and help with the computation.

## References

- [1] G. Gutsev, A. I. Boldyrev, *Chem. Phys.* **1981**, *56*, 277–283.
- [2] G. Gutsev, A. I. Boldyrev, *Adv. Chem. Phys.* **1985**, *61*, 169–221.
- [3] C. Kolmel, G. Palm, R. Ahlrichs, M. Bar, A. I. Boldyrev, *Chem. Phys. Lett.* **1990**, *173*, 151–156.
- [4] G. Gutsev, A. I. Boldyrev, *J. Phys. Chem.* **1990**, *94*, 2256–2259.
- [5] G. Gutsev, A. I. Boldyrev, *Chem. Phys. Lett.* **1983**, *101*, 441–445.
- [6] X.-B. Wang, C.-F. Ding, L.-S. Wang, A. I. Boldyrev, J. Simons, *J. Chem. Phys.* **1999**, *110*, 4763–4771.
- [7] S. Freza, P. Skurski, *Chem. Phys. Lett.* **2010**, *487*, 19–23.
- [8] C. Sikorska, P. Skurski, *Chem. Phys. Lett.* **2012**, *536*, 34–38.
- [9] I. Anusiewicz, *J. Phys. Chem. A.* **2009**, *113*, 6511–6516
- [10] A. I. Boldyrev, J. Simons, *J. Chem. Phys.* **1993**, *99*, 4628–4637
- [11] G. L. Gutsev, P. Jena, H. J. Zhai, L.-S. Wang, *J. Chem. Phys.* **2001**, *115*, 7935–7944.
- [12] I. Swierszcz, I. Anusiewicz, *Chem. Phys.* **2011**, *383*, 93–100
- [13] S. Smuczynska, P. Skurski, *Inorg. Chem.* **2009**, *48*, 10231–10238.
- [14] G. L. Gutsev, B. K. Rao, P. Jena, X. B. Wang, L.-S. Wang, *Chem. Phys. Lett.* **1999**, *312*, 598–605.
- [15] G. L. Gutsev, P. Jena, H. J. Zhai, L.-S. Wang, *J. Chem. Phys.* **2001**, *115*, 7935–7944.

- [16] S. Behera, D. Samanta, P. Jena, *J. Phys. Chem. A* **2013**, 117, 5428-5434.
- [17] C. Paduani, P. Jena, *J. Nanoparticles Research* **2012**, 14, 1035-1043.
- [18] D. Samanta, M. M. Wu, P. Jena, *J. Inorg. Chem.* **2011**, 50, 8918-8925.
- [19] M. Gotz, M. Willis, A. Kandalam, G. G. Gantefor, P. Jena, *Chem. Phys. Chem.* **2010**, 11, 853-858.
- [20] B. Pathak, D. Samanta, R. Ahuja, P. Jena, *Chem. Phys. Chem.* **2011**, 12, 2422-2428.
- [21] M. Willis, M. Gotz, A. K. Kandalam, G. Gantefor, P. Jena, *Angew. Chem. Int. Ed.* **2010**, 49, 8966-8970.
- [22] M. Marchaj, S. Freza, O. Rybacka, P. Skurski, *Chem. Phys. Lett.* **2013**, 574, 13-17.
- [23] D. Samanta, P. Jena, *J. Am. Chem. Soc. (communications)* **2012**, 134, 8400-8403.
- [24] P. Jena, *J. Phys. Chem. Letters* **2013**, 4, 1432-1442.
- [25] H-J. Zhai, J. Li, L-S. Wang, *J. Chem. Phys.* **2004**, 121, 8369-8374.
- [26] A. W. Hofmann, *Proceedings of the Royal Society.* **1855**, 8, 1-3.
- [27] P. v. R. Schleyer, *Chemical Reviews.* **2001**, 101, 1115-1118.
- [28] E. Hückel, *Z. Phys.* **1931**, 70 204-86.
- [29] W. V. E. Doering, F. L. Detert, *J. Am. Chem. Soc.* **1951**, 73, 876-877.
- [30] A. Hirsch, Z. Chen, H. Jiao, *Angew. Chem., Int. Ed. Engl.* **2000**, 39, 3915-17.
- [31] A. I. Boldyrev, L-S. Wang, *Chem. Rev.* **2005**, 105, 3716-3757.
- [32] I. Nenner, G. J. Schulz, *J. Chem. Phys.* **1975**, 62, 1747-1758.
- [33] P. C. Engelking, W. C. Lineberger, *J. Chem. Phys.* **1977**, 67, 1412-1417.
- [34] A. Becke, *J. Chem. Phys.* **1993**, 98, 5648-5652.
- [35] C. Lee, W. Yang, R. Parr, *Phys. Rev. B* **1988**, 37, 785-789.
- [36] M. J. Frisch, G. W. Trucks, H. B. Schlegel, G. E. Scuseria, M. A. Robb, J. R.

Cheeseman, G. Scalmani, V. Barone, B. Mennucci, G. A. Petersson, *et al.* *Gaussian 09, Revision B.01*, Gaussian, Inc., Wallingford CT **2010**.

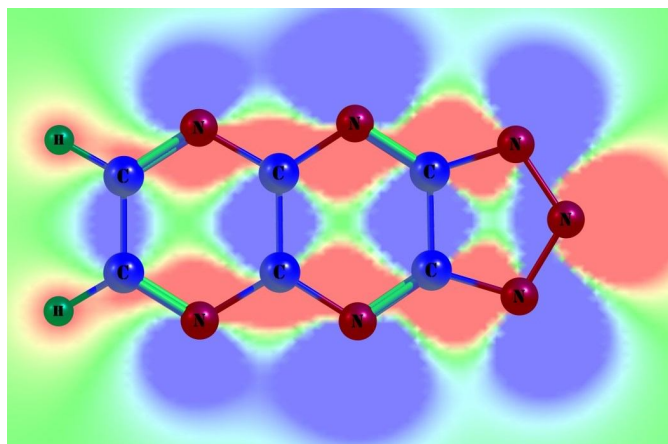
[37] P. v. R. Schleyer, C. Maerker, A. Dransfeld, H. J. Jiao, N. J. r. V. E. Hommes, *J. Am. Chem. Soc.* **1996**, *118*, 6317–6318.

[38] P. v. R. Schleyer, H. J. Jiao, N. J. r. V. E. Hommes, V. G. Malkin, , O. L. Malkina, *J. Am. Chem. Soc.* **1997**, *119*, 12669–12670.

[39] NIST Chemistry Webbook. <http://webbook.nist.gov/chemistry/> (Aug 2, 2013).

[40] J. M. Gonzales, C. J. Barden, S. T. Brown, P. v. R. Schleyer, H. F. Schaefer III, Q-S. Li, *J. Am. Chem. Soc.* **2003**, *125*, 1064-1071.

## TOC



## Supplemental Information





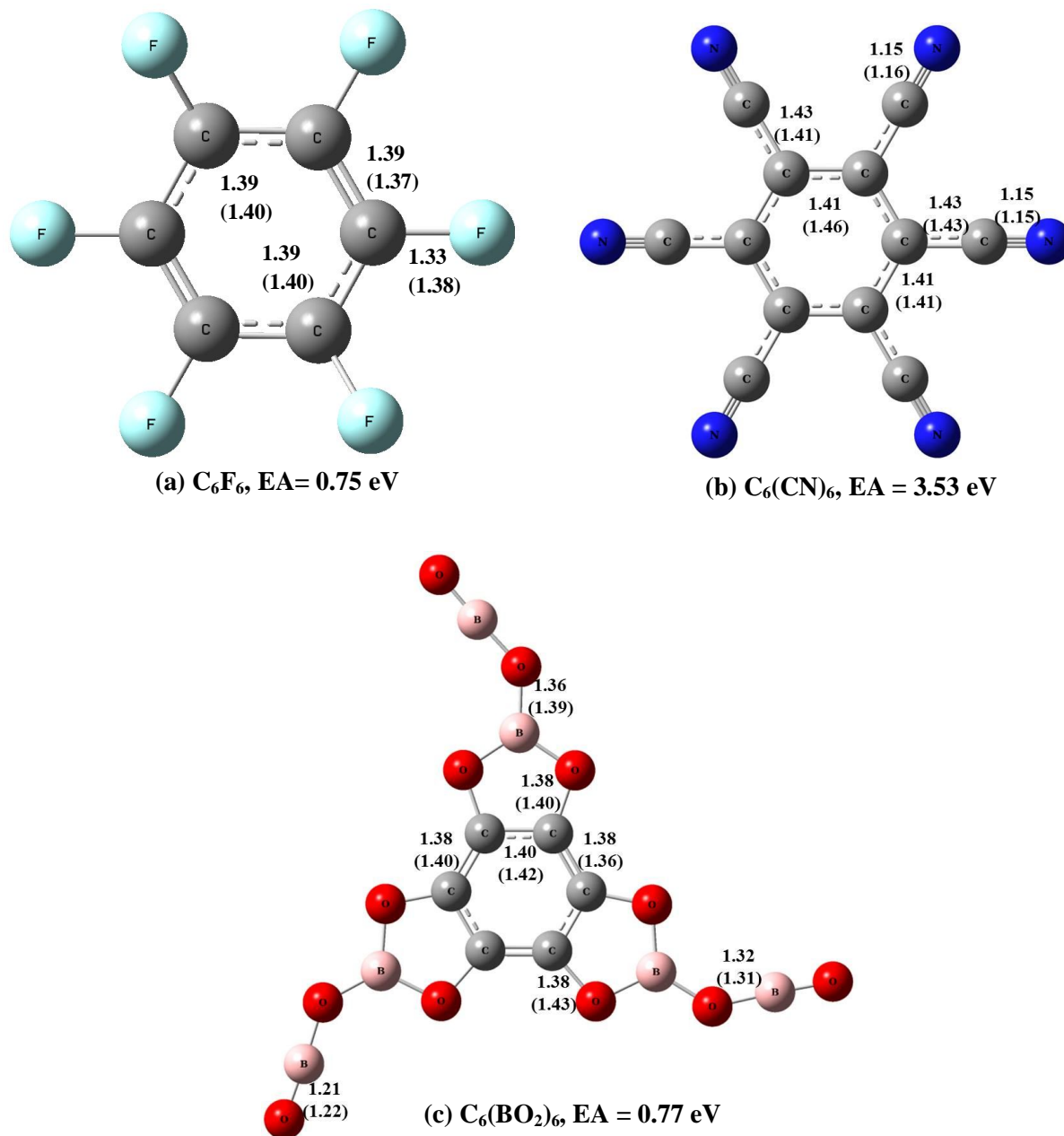


Fig. 2: Equilibrium geometries of the ground state of neutral and anionic  $C_6X_n$  ( $n=6$ ;  $X=F, CN, BO_2$ ). The bond lengths are given in Å. The bond lengths in brackets are those of the anion.

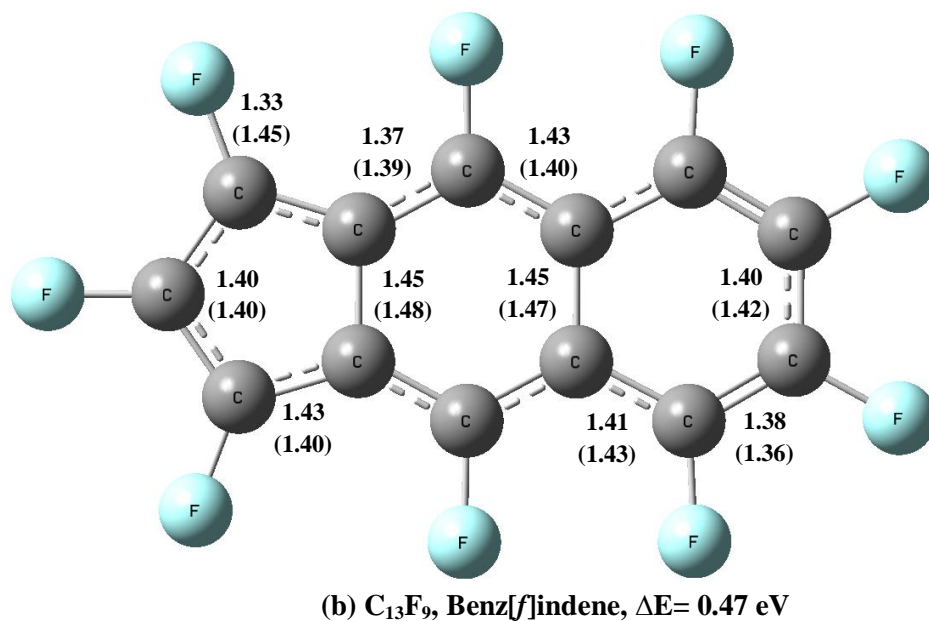
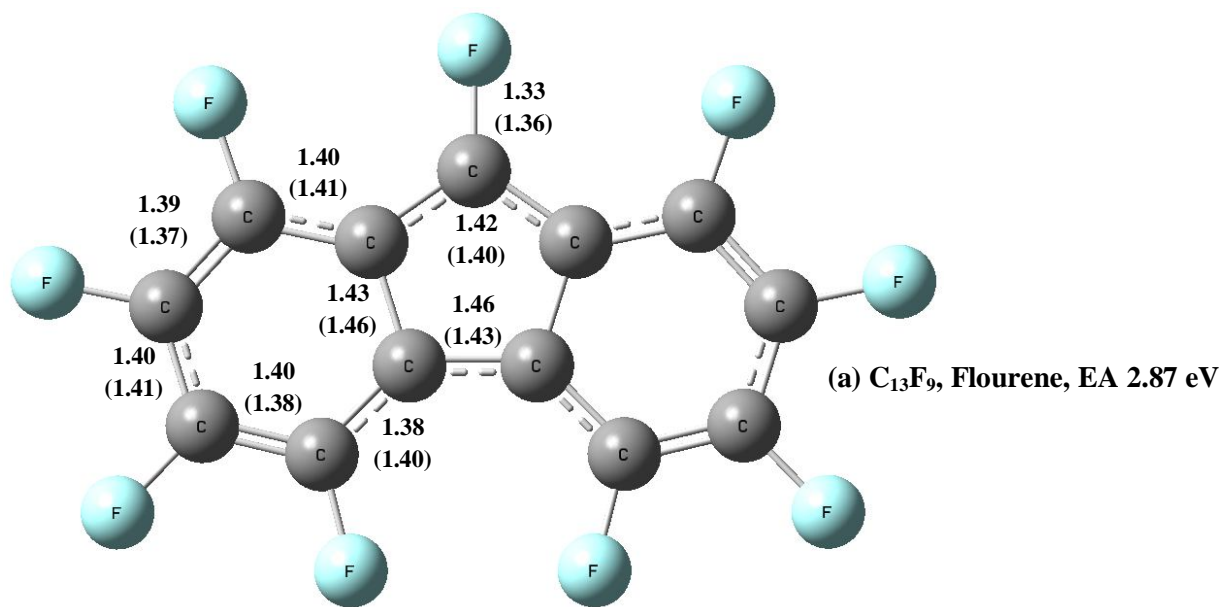


Fig. 3: Geometries of  $C_{13}F_9$ . The bond lengths are given in Å. The bond lengths in brackets are those of the anion.

Fig. 3 presents the geometries of the ground state and first isomer of neutral  $C_{13}F_9$ . The flourene structure is the ground state geometry with benz[f]indene being the higher energy isomer.  $\Delta E$  corresponds to the energy difference between the ground state and higher energy isomer. Here we can see that the highest EA attained is that of the benz[f]indene structure at 2.98 eV, which is significantly less than the same structure with chemical formula  $C_4N_9$  which has an EA of 4.58 eV, a difference of 1.60 eV.

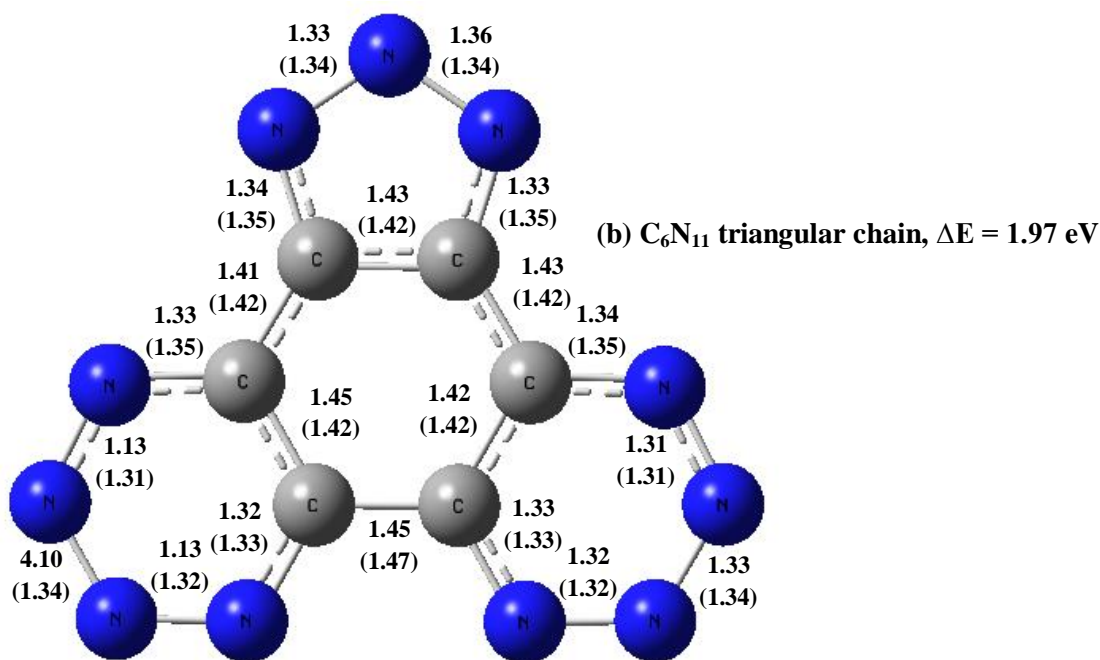
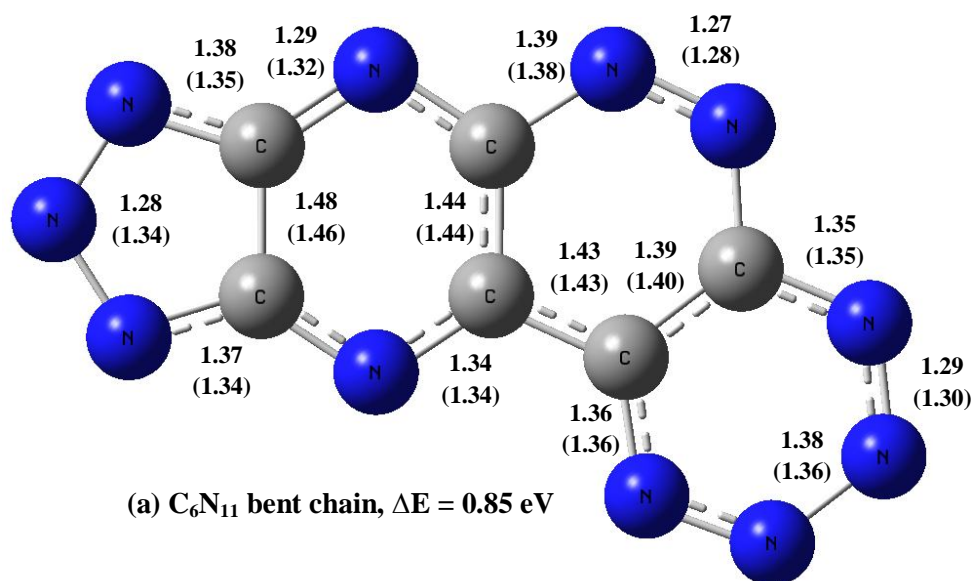


Fig. 4: Geometries of  $C_6N_{11}$ . The bond lengths are given in Å. The bond lengths in brackets are those of the anion.

Fig. 4 shows the isomers of  $C_6N_{11}$ . Fig. 3(a) is a bent chain which is 0.85 eV higher in energy than the ground state. Its EA is 5.22 eV, only 0.01 eV different from the EA of the ground state. Exploration into longer bent chains further increased the  $\Delta E$  between the linear ground state and the bent isomer. Fig. 3(b) is a triangular chain whose total energy is 1.97 eV

higher than the ground state. Its EA is 4.36 eV. The anion structure is symmetric. The neutral, however, breaks this symmetry as the middle N-N bond on one of the six-membered rings splits, separating the nitrogen to a distance of 4.1 Å, with a bond angle of 178° to the carbon for each branch. Subsequently, the remaining nitrogen bonds on that ring become triple bonds with a length of 1.13 Å. The other six-membered ring remains mostly unchanged. This does cause some contortions in the near side of the five-membered ring. The significant difference between the anion and neutral geometries leads to a VDE of 5.95 eV. This bond splitting of the nitrogen end on one of the rings continues to occur in larger chains as well, which continue to be less stable than the linear counterparts at larger sizes.

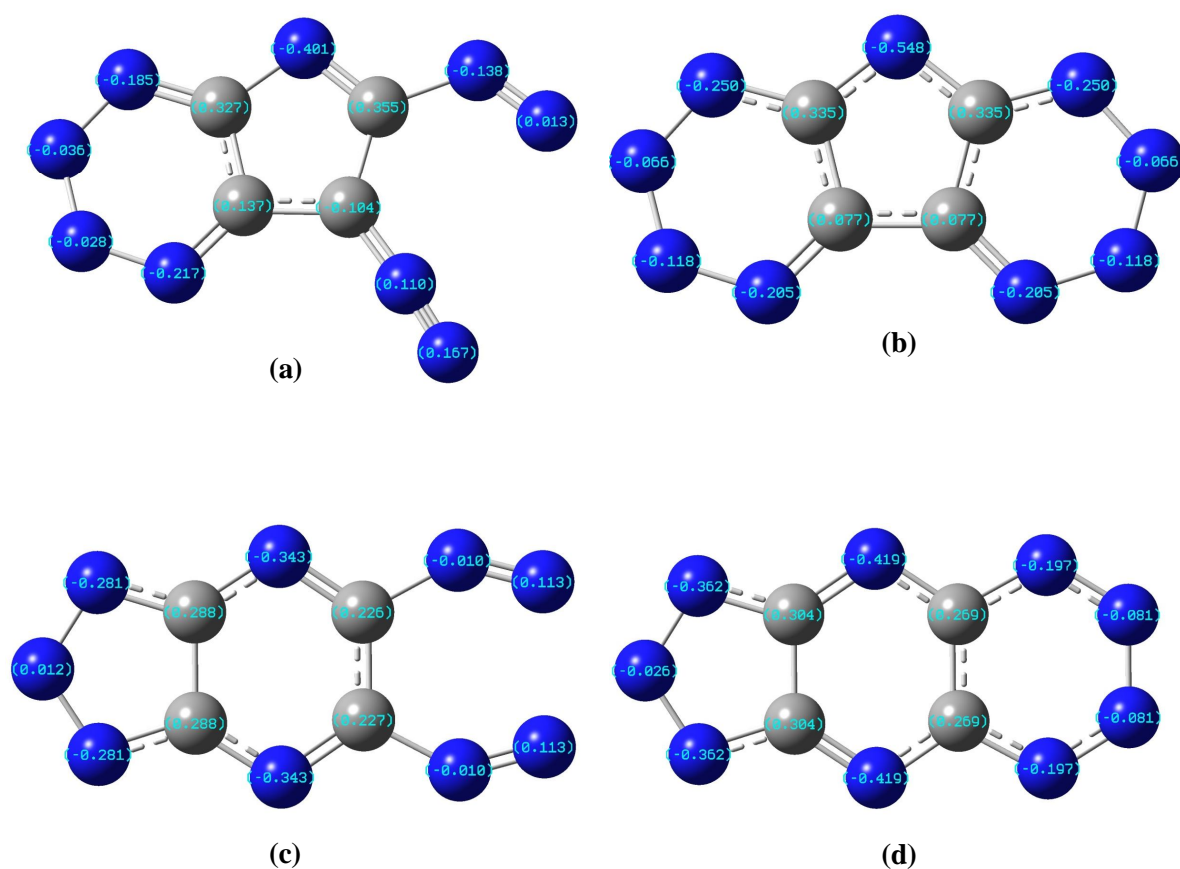
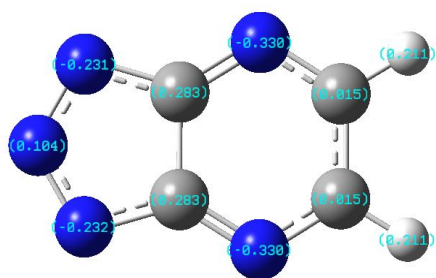


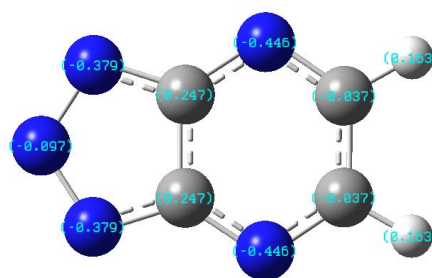
Fig. 5: NBO charge distribution of  $C_4N_9$  for both the fluorene and benz[f]indene structures. The neutral structure is on the left, the anion structure on the right.

Fig. 5 shows the NBO charge distribution for  $C_4N_9$ . For neutral fluorene in Fig. 4(a), the four carbon atoms as well as the nitrogen atoms located at the end sites of the split ring carry a positive charge, while rest of the nitrogen atoms carry negative charge. Overall the most charge is found on the nitrogen atom at the tip of the five-membered ring, namely -0.40 and its neighboring carbon atoms carry charge of 0.33, and 0.36. Moving to the anion (Fig. 4(b)) the most significant changes occur with the creation of a bond between the separated nitrogen atoms,

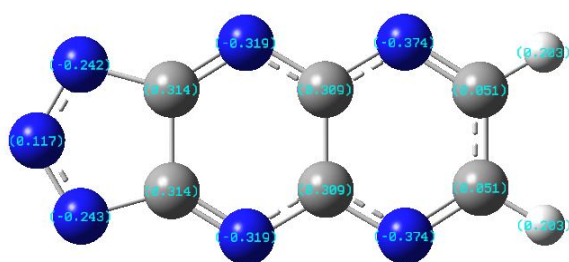
with the participating nitrogen atoms and their nearest neighbors gaining some of the negative charge originating from the added electron. The largest change in charge occurs at the nitrogen atom at the tip of the five-membered ring (from -0.40 to -0.55), though its nearest neighbors are unaffected. The neutral cluster with the benz[*f*]indene structure (Fig. 4(c)) carries 0.23-0.29 charge on the four carbon atoms. Unlike the fluorene structure all nitrogen atoms here do not have a negative charge. The tip of the five-membered ring is closest to being neutral, with a charge of 0.01, and the N atoms at the far end or the last six-membered ring have charges of 0.11. The nearest neighbors of the N atom at the tip of the five-membered ring carry a negative charge of -0.28, and the N atoms on the center six-membered ring carries the largest charge of -0.34. The added electron in the anion (Fig 4. (d)) can be found to be distributed mostly on the four N atoms on the last six-membered ring, from -0.01 to -0.20 and from 0.11 to -0.08. The nitrogen on the center six-membered ring as well as the nearest neighbors on the five-membered ring also gained some charge. Here the nitrogen at the tip of the five-membered ring gained the least charge, from 0.01 to -0.03. The positive charge of the four carbon increased by a minor amount as well.



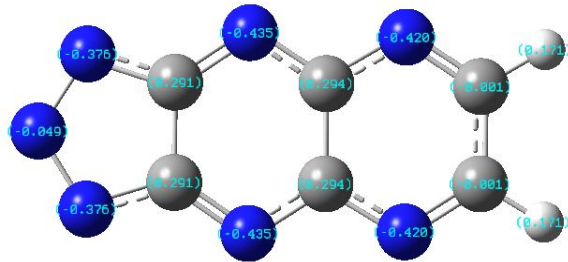
(a)



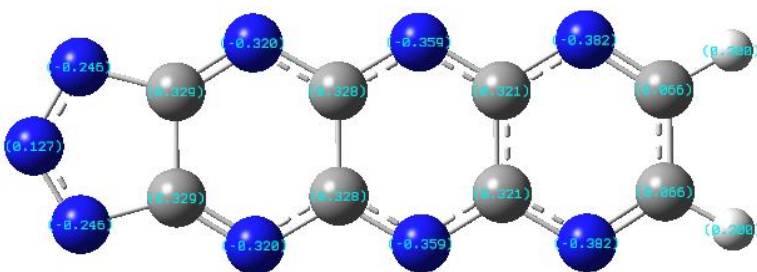
(b)



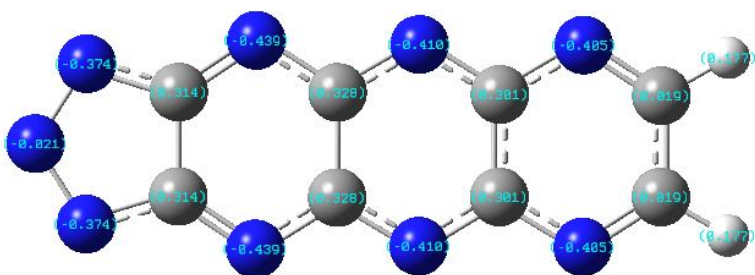
(c)



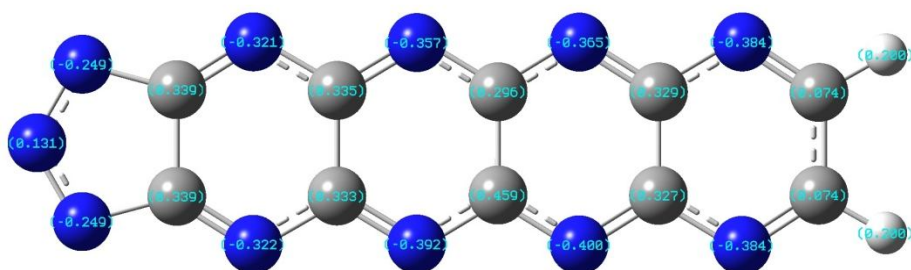
(d)



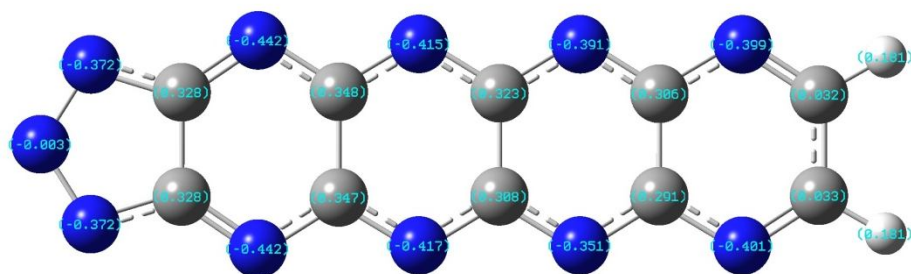
(e)



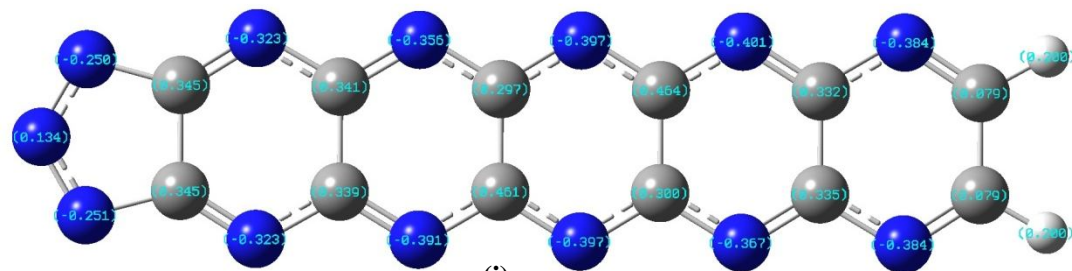
(f)



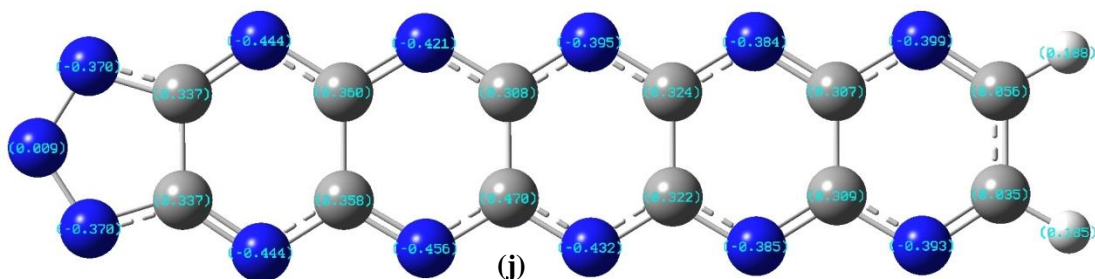
(g)



(h)



(i)



(j)

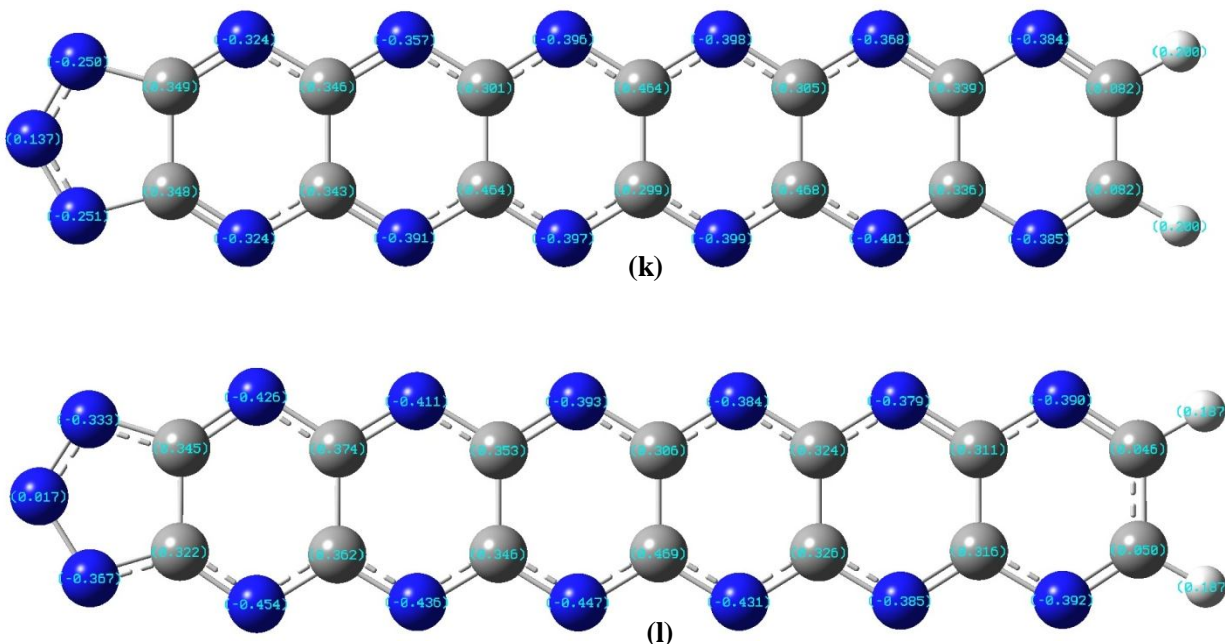


Fig. 6: NBO charge distribution of polycyclic aromatic hydrocarbons from 1-6 benzene. The neutral structures are shown first, the anion structures second.

Fig. 6 shows the NBO charges for the structures with 1-6 six-membered rings. A general trend can be seen in the charge distribution of all of these molecules. For the neutral all the carbon atoms maintain a positive charge with the largest charge on the C nearest the middle of the structure, and the smallest on the C attached to the H. The N on the tip of the five-membered ring carries a positive charge, while the rest of the N atoms have negative charge. The largest charge is seen on the N on the six-membered ring at the end of the structure for (a), (c), and (e). For (g), (i), and (k) the charge is asymmetric at top and bottom with the largest charge found on one of the N atoms on the second to last six-membered ring. The negative charge decreases as we move toward the five-membered ring. For the anion the charges on the C atoms are mostly unchanged from the neutral. The N atom on the tip of the five-membered ring becomes slightly negative to effectively neutral and the rest of the N atoms gain negative charge. The trend in the anion reverses however, compared to the neutral. In the anion the largest charge (and therefore the largest gain) is found on the N atom in the six-membered ring attached to the five-membered ring with the charge diminishing on subsequent nitrogen as we move away.